Correlation between 3-MCPD-induced organ toxicity and oxidative stress response in male mice

Schultrich, Katharina; Henderson, Colin J.; Braeuning, Albert; Buhrke, Thorsten

Published in:
Food and Chemical Toxicology

DOI:
10.1016/j.fct.2019.110957

Publication date:
2020

Correlation between 3-MCPD-induced organ toxicity and oxidative stress response in male mice

Katharina Schultrich[1], Colin J. Henderson[2], Albert Braeuning[1], Thorsten Buhrke[1]*

[1] German Federal Institute for Risk Assessment, Department of Food Safety, Max-Dohrn-Str. 8-10, 10589 Berlin, Germany

[2] School of Medicine, Ninewells Hospital and Medical School, University of Dundee, Dundee, DD1 9SY, United Kingdom

* Corresponding author:

Dr. Thorsten Buhrke

German Federal Institute for Risk Assessment

Department of Food Safety

Max-Dohrn-Str. 8-10

10589 Berlin

Germany

Phone: ++49 30 18412-3221

E-Mail: thorsten.buhrke@bfr.bund.de

Highlights

- The transgenic HOTT reporter mouse was employed to examine 3-MCPD-mediated induction of oxidative stress
- 3-MCPD induces oxidative stress in mouse kidney, testes and brain
- 3-MCPD leads to the irreversible oxidation of the redox sensor protein DJ-1
- 3-MCPD does not severely affect Nrf2-dependent gene expression in different mouse organs

Abstract

3-Chloro-1,2-propanediol (3-MCPD) is a food contaminant which has been classified as a non-genotoxic carcinogen (category 2B). Previous studies suggested that oxidative stress might play a role in 3-MCPD toxicity. To elucidate the impact of 3-MCPD-mediated organ toxicity in more detail, transgenic reporter mice were employed which contain a *lacZ* reporter under the control of the heme oxygenase 1 (*Hmox1*) promoter which is responsive to oxidative stress. The mice received daily doses of up to 100 mg/kg body weight 3-MCPD per day in a 28-day feeding study. Subsequently, tissue slices from different organs were subjected to X-Gal staining as the readout for *lacZ* gene expression. A dose-dependent increase of blue stain was observed in mouse kidney that was exclusively visible in the renal cortex but not in the renal medulla. Moreover, blue-stained regions were detected in the basal membrane of the seminiferous tubules in testes and also in specific brain regions (cerebellum, midbrain and pons). Notably, gene expression of a number of Nrf2-dependent target genes except *Hmox1* was not severely affected by 3-MCPD. In all three organs, however, the amount of irreversibly oxidized DJ-1 protein, which is a biomarker for oxidative stress, was significantly increased already by low doses of 3-MCPD.

Keywords: 3-MCPD, organ toxicity, oxidative stress, Hmox1 activation

Introduction

Fatty acid esters of 3-Chloro-1,2-propanediol (3-MCPD) are heat-induced food process contaminants that are predominantly formed during the refinement of vegetable oils and fats (Craft et al. 2013; Kuhlmann 2011). After ingestion with food, the esters are nearly quantitatively hydrolysed in the gastrointestinal tract, thereby liberating free 3-MCPD (Abraham et al. 2013; Barocelli et al. 2011). The free compound is readily resorbed into the body and partially excreted with the urine. 3-MCPD is metabolized i) to its oxidation product β-chlorolactic acid and ii) to dihydroxypropylmercapturic acid (DHPMA) which is the terminal product of an initial 3-MCPD glutathione conjugate. As for non-modified 3-MCPD, both metabolites are also excreted with urine (Barocelli et al. 2011; Jones et al. 1978).

3-MCPD has been classified to be non-genotoxic and possibly carcinogenic to humans (category 2B; (IARC 2012). In long-term feeding studies, repeated oral application of 3-MCPD at doses as low as 2 mg/kg b.w./day caused nephrotoxicity (tubular hyperplasia), testicular toxicity (atrophy and arteritis) in male rats, and nephrotoxicity in female rats. Moreover, an increased incidence for Leydig cell tumors and kidney tubular adenoma were observed (Cho et al. 2008). The underlying molecular mechanisms that are associated with the carcinogenic potential of 3-MCPD, however, are barely known. To unravel the molecular toxicity mechanism(s) of 3-MCPD, a 28-day feeding study with rats was conducted followed by the analysis of proteomic and transcriptomic alterations induced by 3-MCPD in different rat organs. Bioinformatic evaluation of these proteomic and transcriptomic data revealed that 3-MCPD induced oxidative stress and affected glutathione metabolism in rat kidney and testes and inhibited glycolysis in rat testes (Buhrke et al. 2017; Sawada et al. 2015; Sawada et al. 2016). In a more detailed analysis, the redox sensor protein DJ-1 was identified to be a sensitive biomarker for 3-MCPD-mediated oxidative stress (Buhrke et al. 2018).

In the present study, so-called HOTT reporter mice were employed to study the impact of 3-MCPD on oxidative stress response *in vivo* in more detail. In the transgenic HOTT mice, the bacterial *lacZ* gene encoding β-galactosidase is under the control of the heme oxygenase 1

(*Hmox1*) promoter. The *Hmox1* promoter is activated by pro-oxidant stimuli, predominantly via the Nrf2 transcription factor. Oxidative stress-mediated *Hmox1* promoter activation induces *lacZ* gene expression. β-galactosidase activity can then easily be visualized by using the common X-Gal staining, and blue-colored regions in X-Gal-stained organ slices indicate a high burden of oxidative stress in these regions (McMahon et al. 2018). Thus, the use of HOTT reporter mice in the present study was a straight-forward approach to identify the organs that were affected by 3-MCPD-mediated oxidative stress and to study the oxidative stress response in these organs in detail.

Materials and Methods

Animal study

The animal work in this study was carried out under the Animals (Scientific Procedures) act (1986) and EU Directive 2010/63/EU after approval by the Welfare and Ethical treatment of Animals Committee of the University of Dundee and the University Veterinary Surgeon. The heterozygous heme oxygenase triple transgenic (HOTT) reporter mice on a C57BL/6NTac background were supplied by the Medical School Resource Unit, University of Dundee (McMahon et al. 2018).

20 young adult (16-20 weeks, n=5) male mice, weighting ~ 25 g, were randomly allocated to four groups. Group 1 served as vehicle control and was treated with water by oral gavage, daily for 28 days. Animals of groups 2, 3 and 4 received 1, 10 and 100 mg 3-MCPD (Sigma-Aldrich, Munich, Germany) per kg body weight for 28 days, respectively, by oral gavage.

Animals were housed in open-top cages with *ad libitum* access to food (RM1, Special Diet Services, Essex, UK) and water. Mice were held at 12 h light/dark environment with temperature between 20 - 24°C and relative humidity between 45 - 65%.

Animals were euthanized by a rising concentration of CO_2 and death was confirmed by exsanguination. ~~The organs k~~Kidney, testes, ~~and~~ brain, liver, heart and spleen were harvested, individually weighed and cut. Half a medium lobe of the liver was fixed in 10 % neutral buffered formalin and the other half in 1 % paraformaldehyde. For all other organs, ~~O~~one half was snap-frozen and stored at -80°C, and the second half was fixed with Mirsky's fixative (National Diagnostics, Atlanta, USA) overnight at 4°C, and afterwards all tissues were washed in PBS containing 2 mM $MgCl_2$, dehydrated in 30 % sucrose and embedded in Shandon M-1 Embedding Matrix (Thermo Fisher Scientific, Waltham, USA) in a dry ice–isopentane bath. The organs were cut at 10 µm thickness on an OFT5000 cryostat (Bright Instrument Co., Luton, UK) at -20°C.

Organs from Group 4 mice were removed post mortem, rinsed in ice-old sterile PBS and fixed in 4% (w/v) formaldehyde (Gurr; VWR, UK) overnight before being transferred into 70%

(v/v) ethanol. The next day, tissues were dehydrated (Shandon Citadel 1000, Thermo Scientific, UK), and embedded in paraffin wax (Shandon Histocentre 3, Thermo Scientific, UK).

Histochemical analysis

LacZ staining

Slides with 10 µm tissue slices were placed in a staining tray and allowed to equilibrate to room temperature, and then rehydrated in PBS supplemented with 2 mM $MgCl_2$ for 5 min. The slices were entirely covered with X-Gal staining solution (PBS (pH 7.4) including 2 mM $MgCl_2$, 0.01% (w/v) sodium deoxycholate, 0.02% (v/v) Igepal CA630, 5 mM potassium ferricyanide, 5 mM potassium ferrocyanide and 1 mg/ml X-Gal [5-bromo-4-chloro-3-indolyl β-D-galactopyranoside]) and incubated in a humidified chamber at 37°C overnight. The next day, slides were washed with PBS and counterstained with Nuclear Fast Red (Vector Laboratories, Burlingame, USA). Subsequently, organ slices were washed twice with double-distilled water and dehydrated with 70 % ethanol followed by 95 % ethanol and incubated in Histoclear (VWR, Radnor, USA) for 3 min. After air-drying, coverslips were applied by using DPX mountant (Sigma-Aldrich, Munich, Germany).

Densitometric evaluation

The software ZEN 2.3 lite blue edition (Carl Zeiss Microscopy, Thornwood, USA) was used for quantitative image analysis of the X-Gal staining. The densitometric analysis was based on microscope images which were acquired with a Zeiss Axio Observer (Carl Zeiss, Jena, Germany). The images were analyzed by using a customized automatic segmentation algorithm for each image. For the automatic segmentation a threshold for the red, green and blue (RGB) channels was defined in order to filter the area of blue coloration within the image. The value of each RGB channel of each pixel had to be below the threshold to remove the background in each image and to quantify the corresponding pixels as X-Gal positive. For image analysis, the following segmentation parameters were used: smooth:

none; sharpen: none; minimum area: 1; threshold: red 0-1468, green 0-1366, blue 0-1839; tolerance: 3 %; neighborhood: 1; separate: morphology; count: 3. After the software automatically determined the area of blue coloration within the microscopic image, the total area of the image was set in relation to the area of the measured blue staining. Subsequently, the percentage of the area of X-Gal positive staining of each acquired microscope image was determined. For the kidney cortex and testes, five images were analyzed for each animal whereas three images were analyzed for midbrain, cerebellum and pons for each animal.

Protein extraction and Western blotting

For protein extraction, 50-60 mg of frozen tissue from mouse kidney, testes or brain was disrupted in the presence of liquid nitrogen by using mortar and pestle. The frozen tissue powder was suspended in lysis buffer (50 mM Tris-HCl (pH 7.5), 150 mM NaCl, 2 µM EGTA, 0.1 % (w/v) SDS, 0.5 % (w/v) deoxycholic acid, 2 % complete protease inhibitor cocktail 1x (Roche, Basel, Switzerland)) and further homogenized by stepwise sonification. The protein extract were centrifuged at 20,000 x g for 30 min at 4°C, and the supernatant was stored at −80 °C. The protein content was determined by using the Bicinchoninic Acid Kit for Protein Determination (Sigma-Aldrich, Munich, Germany).

2DE Western blotting

2D gel electrophoresis was performed according to (Buhrke et al. 2018) with the modification that the Ettan IPGphor IEF separation unit (GE Healthcare, Freiburg, Germany) was used as follows: 300 V for 1 h, gradient from 300 to 1000 V within 1 h, gradient from 1000 to 5000 V within 2 h, and finally 5000 V for 1.5 h. The polyacrylamide gel electrophoresis was conducted according to the protocol of (Laemmli 1970) by using a 12 % polyacrylamide gel.

2D gels were blotted according to (Scharmach et al. 2012) by using a rabbit monoclonal antibody raised against PARK7/DJ1 (ab76008; Abcam, Cambridge, UK) in 1:5000 dilution, and goat-anti-rabbit-IgG-HRP (HAF008, R&D systems, Minneapolis, Canada) in a 1:2000

dilution as secondary antibody. For acquisition of the chemiluminescent Western blot a VersaDoc MP4000 Imaging System was used (Bio-Rad, Munich, Germany).

Densitometric analysis of the spot intensities from the 2D-Western blots was carried out by using the Image Lab 5.2 software (Bio-Rad, Munich, Germany). Spot intensities were compared to the intensities of the other spots on the same blot and expressed as relative intensities.

1D Western blotting

1D Western blotting for detection of 4-HNE protein adducts was carried out and detected as described above (Laemmli 1970; Scharmach et al. 2012). 20 µg of protein per lane and a 12 % polyacrylamide gel was used for the electrophoretic separation. The Western blotting was conducted by using rabbit polyclonal antibody against 4-HNE (ab46545, Abcam, Cambridge, UK) in a 1:1000 dilution and a goat-anti-rabbit-IgG-HRP (HAF008, R&D systems, Minneapolis, Canada) in a 1:5000 dilution as secondary antibody. For restaining of glyceraldehyde-3-phosphate dehydrogenase (GAPDH) as loading control, the primary and secondary antibodies of 4-HNE detection were removed from the blot membrane by incubating the membrane for 30 minutes at 55°C in stripping solution pH 6.7 (62 mM Tris-HCl, 5 % SDS and 0.88 % β-mercaptoethanol) with agitation. After washing the membrane with TBST for 10 minutes the restain of GAPDH was carried out using mouse monoclonal antibody against GAPDH (ab8245, Abcam, Cambridge, UK) in a 1:7500 dilution and a secondary goat-anti-mouse-IgG-HRP antibody (A-014HRP, Seramun Diagnostica, Heidesee, Germany) in a 1:10000 dilution. Detection and densitometric analysis was carried out as described above. Single band intensities were compared to the intensities of the entire lane and expressed as relative intensities in relation to GAPDH.

RNA isolation and quantitative real-time RT-PCR

Total mRNA was extracted from all animals of Group 1, 2 and 3. After disruption of 15-30 mg frozen tissue by a mortar and pestle in liquid nitrogen, the RNA was homogenized and

isolated by using the RNeasy Mini Kit (Qiagen, Hilden, Germany). The organs from Group 4 were formalin-fixed and paraffin-embedded. The extraction of total mRNA from these tissues was done by using the RNeasy FFPE Kit (Qiagen, Hilden, Germany). The concentration of RNA was determined with a NanoDrop ND-1000 spectrometer (NanoDrop Technologies, Wilmington, DE, USA).

The isolated mRNA samples were reverse transcribed by using the high capacity cDNA reverse transcription kit (Applied Biosystem/ Life Technologies GmbH, Darmstadt, Germany). Afterwards, the cDNA was subjected to PCR analysis via Maxima SYBR Green/Rox qPCR Master Mix (Thermo Fisher Scietific, Waltham, MA, USA) and a Stratagene MX3005P real-time PCR cycler according to the protocol by (Luckert et al. 2013). Gene expression was calculated by relative quantification according to the ΔΔCt method and normalization with β-actin as reference gene.

The following primer were used: β-Actin 5'-GATCATTGCTCCTCCTGAGC-3' (forward) and 5'-CATCGTACTCCTGCTTGCTG-3', glutathione S-transferase P1 (*Gstp1*) 5'-ATATGTCACCCTCATCTACACCA-3' (forward) and 5'-CTGGTCACCCACGATGAAAG-3' (reverse), catalase (*Cat*) 5'-CAATGGCAATTACCCGTCCTG-3' (forward) and 5'-TAGTCCTTGTGAGGCCAAACC-3' (reverse), superoxide dismutase 1 (*Sod1*) 5'-GGGTTCCACGTCCATCAGTAT-3' (forward) and 5'-CCTTTCCAGCAGTCACATTGC-3' (reverse), protein deglycase (*Park7*) 5'- GCTCTGTTGGCTCACGAAGT-3' (forward) and 5'TCCTTAGCCAGTGGGTGTGT-3' (reverse), heme oxygenase 1 (*Hmox1*) 5'-GCAGAACCCAGTCTATGCCC-3' (forward) and 5'- GGCGTGCAAGGGATGATTTC-3' (reverse), glutaredoxin 1 (*Glrx1*) 5'-CTCACCGGAGCGAGAACAG-3' (forward) and 5'-TCTGCTTCAGCCGAGTCATC-3' (reverse), glutaredoxin 2 (*Glrx2*) 5'-ACAAGGCTGTGGAGTTGGAT-3' (forward) and 5'-GCTGCGCCTCCAATAAATCG-3' (reverse), peroxiredoxin 1 (*Prdx1*) 5'-AGTGATTGGCGCTTCTGTGG-3' (forward) and 5'-AATGGTGCGCTTGGGATCTG-3' (reverse), peroxiredoxin 6 (*Prdx6*) 5'-CAGGGACCTTGCCATCCTTT-3' (forward) and 5'-AGGCATGTTGTTAGCGTCCT-3' (reverse), sulfiredoxin 1 (*Srxn1*) 5'-TACCAATCGCCGTGCTCATC-3' (forward) and 5'-

AGTAGTAGTCGCCACCCTGG-3’ (reverse), glutathione reductase (*Gsr*) 5’-CGAGGAACTGGAGAATGCCG-3’ (forward) and 5’-TCTGGAATCATGGTCGTGGTG-3’ (reverse), glutamate-cysteine ligase catalytic subunit (*Gclc*) 5’-TGACATCGACCTGACCATCG-3’ (forward) and 5’-AACGTGCTGTGCCAGAAGAT-3’ (reverse), glutathione synthetase (*Gss*) 5’-ATGCGGTGGTGCTACTGATT-3’ (forward) and 5’-TACGGCACGCTGGTCAAATA-3’ (reverse).

Statistics

Statistical analysis was carried out using the One Way Analysis of Variance (ANOVA) followed by Dunnett’s multiple comparison tests. Statistical significance was assumed at $p<0.05$.

Results

To examine which organs are predominantly affected by 3-MCPD-induced oxidative stress, HOTT reporter mice were daily treated with 3-MCPD for 28 days. One animal of the control group (Group 1) was found dead at day 7, and the organs of this mouse were not preserved for further analysis. Thus, the control group consisted of four animals whereas the three treatment groups consisted of five animals each. The mice of the high dose group (100 mg 3-MCPD/kg b.w./day; Group 4) had to be euthanized at day 7 due to severe weight loss (> 20%) and an overall bad constitution of all five animals. Thus, it has to be noted that all results regarding the high dose group have been obtained from mice showing signs of acute toxicity at sacrifice after 7 days of 3-MCPD treatment, whereas the animals of the other groups showed no clinical symptoms or signs of acute toxicity and were sacrificed after 28 days of 3-MCPD treatment. Following the animal weights, the mice of the low and the medium dose groups displayed weight curves within the treatment period of 28 days comparable to the mice of the control group whereas the mice of the high dose group lost weight until they had to be euthanized at day 7 (Fig. 1a). No gross phenotypic anomalies were recorded. Regarding the organ to body weight ratios, increased relative weights were observed for kidney, brain and heart of the animals of the high dose group and for the hearts of the animals of the medium dose group. The organ to body weight ratios ~~for liver and testes~~of other organs were not affected upon 3-MCPD treatment (Fig. 1b).

Microscopic slices were prepared from different organs of the HOTT mice and subjected to X-Gal staining. Strong blue stain was observed for the entire kidney cortex from the mice of the high dose group compared to the control group (Fig. 2a). As the *lacZ* gene in the HOTT reporter mice is under the control of the ROS-sensitive *Hmox1* promoter, blue-colored regions are indicative for a high ROS burden in the respective organ (McMahon et al. 2018). Thus, the animals of the high dose group were suffering from severe oxidative stress in their kidneys. Moreover, the X-Gal staining was more intense in the seminiferous tubules of the testes of the mice from the high dose group compared to the control group (Fig. 2b). Finally,

specific regions of the brains of the mice from the high dose group, namely cerebellum, midbrain and pons, were clearly stained blue whereas there was almost no stain visible in the brains of the control mice (Fig. 2c). Compared to these strong effects in the organs from the mice of the high dose group, the effects observed in the organs from the animals of the low dose and medium dose groups were more moderate (Fig. 3a). Indeed, densitometric evaluation of the X-Gal staining revealed that a statistically significant dose-dependent increase of the blue color was only observed for the kidney (Fig. 4a). With respect to testes and brain, a significant increase of X-Gal-positive cells was only observed for the animals from the high dose group (Fig. 4b-e). In contrast to kidneys, testes and brain, no dose-dependent increase of the X-Gal staining was visible in liver, heart and spleen (data not shown). Regarding X-Gal staining in kidney cortex, a more detailed inspection revealed that blue stain first appeared in the glomeruli whereas kidney tubules were stained only at higher 3-MCPD doses (Fig. 3b).

To evaluate a potential oxidative stress response in the different mouse organs at the molecular level, the impact of 3-MCPD on gene expression of a number of Nrf2-dependent genes was examined. Nrf2 is a transcription factor that is activated under oxidative stress conditions and that promotes gene expression of a number of genes whose products have a function in ROS detoxification (Chen and Kunsch 2004). Gene expression of *Gstp1*, *Cat*, *Sod1*, *Park7*, *Hmox1*, *Glrx2*, *Prdx1*, *Prdx6*, *Gclc* and *Gss* was only slightly stimulated by 3-MCPD in mouse kidney with the strongest effects being observed for the high dose group. Notably, *Sod1*, *Glrx2* and *Gss* gene expression was significantly decreased in the kidneys of the mice from the high dose group (Fig. 5a). In mouse testes and brain, 3-MCPD hardly affected gene expression of the Nrf2-dependent genes examined in this study (Fig. 5b-c). A significant induction was only observed for *Gss* in testes and brain and for *Hmox1* in the brains of the animals from the high dose group, however, gene expression of *Gstp1*, *Sod1*, *Glrx1*, *Glrx2*, *Prdx1*, *Srxn1* and *Gsr* was significantly downregulated in testes and brain from the animals of the high dose group. Taken together, there was no strong and no clear dose-

dependent effect of 3-MCPD on the expression of several genes associated with the Nrf2 pathway in mouse kidney, testes and brain.

In a previous study, oxidation of the redox sensor protein DJ-1 (Park7) was shown to be a sensitive biomarker for 3-MCPD-induced oxidative stress in different rat organs (Buhrke et al. 2018). The irreversible oxidation of a redox-sensitive cysteine residue in DJ-1 to a sulfonic acid under oxidative stress conditions can be monitored by 2D-Western blot experiments. Thus, protein samples from different mouse organs from the present study were subjected to two-dimensional gel electrophoresis, and DJ-1 oxidation was evaluated by 2D-Western blotting. At least six different DJ-1 immunoreactive protein spots (labelled A to F) with spots C and D being the most intense ones have been detected (Fig. 6a). According to the results of the previous study, it can be assumed that spot D represents the non-modified DJ-1 protein with the redox-sensitive cysteine residue in its reduced thiol form whereas spot C represents DJ-1 with a cysteine residue being fully oxidized to a sulfonic acid (Buhrke et al. 2018). Representative 2D-Western blot images obtained with protein samples from mouse kidney, testes and brain are shown in Fig. 6b. Densitometric evaluation of the 2D-Western blot images revealed a significant decrease of the reduced DJ-1 form (spot D) accompanied by a significant increase of the oxidized DJ-1 form (spot C) in kidney, testes and brain of the animals from the low dose and the medium dose groups compared to those from the control group (Fig. 6c). Thus, treatment of the HOTT reporter mice with 3-MCPD led to an irreversible oxidation of the DJ-1 protein. *Park7* gene expression, on the other hand, was hardly affected in mouse kidney and not altered in testes and brain upon 3-MCPD treatment (Fig. 5).

Lipid peroxidation was chosen as an additional endpoint to monitor the oxidative stress response in the different mouse organs. For this purpose, protein samples from these organs were separated by SDS-PAGE and subjected to Western blot analysis by using an antibody raised against protein adducts of 4-hydroxynonenal (4-HNE). These adducts indicate the presence of 4-HNE which is a lipid peroxidation product that is formed in the presence of ROS (Luczaj et al. 2017). 4-HNE-protein adducts were detected in the protein samples

obtained from kidney, testes and brain from all animals from the control group and from the medium dose group (Fig. 7a-c). Densitometric evaluation of the band intensities of these blots revealed that the amount of 4-HNE-protein adducts was not altered in these mouse organs upon 3-MCPD treatment (Fig. 7d). Thus, 3-MCPD treatment did not result in an increase of lipid peroxidation in mouse kidney, testes and brain.

Discussion

The food contaminant 3-MCPD is classified as a non-genotoxic carcinogen with kidney and testes being the main target organs according to the results of different animal studies (EFSA 2016; EFSA 2018). In the past few years, we have conducted a number a proteomic and transcriptomic studies to elucidate the underlying molecular mechanism(s) that are associated with the carcinogenic potential of 3-MCPD. The results of these omics screening approaches pointed to a 3-MCPD-mediated induction of oxidative stress accompanied by a deregulation of glutathione metabolism in rat kidney, testes and liver (Braeuning et al. 2015; Buhrke et al. 2017; Sawada et al. 2015; Sawada et al. 2016). In a more detailed analysis, the redox sensor protein DJ-1 was identified to be irreversibly oxidized in different rat organs when 3-MCPD was administered to the animals (Buhrke et al. 2018). Loss of function of DJ-1 by irreversible oxidation is associated with a number of oxidative stress-related diseases such as Parkinson's disease (Ariga 2015; Wilson 2011), thus, putting the brain also into the focus of our 3-MCPD research in addition to the well-known target organs kidney and testes.

In the present study, we took advantage of the HOTT reporter mice that allow an easy visualization and quantification of oxidative stress responses in various mouse organs. After 3-MCPD administration, clear responses in kidney, testes and brain were observed (Fig. 3) whereas there was no increase in X-Gal-derived blue stain in liver and spleen (data not shown). Strong effects, however, were only observed for the animals of the high dose group. These animals had to be sacrificed after seven days of 3-MCPD administration as they had lost > 20% body weight and showed an overall bad constitution. Thus, 3-MCPD-mediated induction of oxidative stress seems, in most organs, to correlate with acute toxicity rather than with long-term exposure to low doses of the compound. In this context, it has to be noted that the doses of 3-MCPD used in the present study are three to four orders of magnitude above human exposure levels, i.e. the doses consumers regularly ingest with food. The tolerable daily intake was recently set to 2 µg/kg b.w./day, and it was stated that for the general population it is unlikely that this TDI is exceeded (EFSA 2018). Thus, it is

questionable whether oxidative stress responses induced by high doses of 3-MCPD as observed in this study are relevant for human health at normal dietary exposure.

X-Gal staining of tissue slices from HOTT mice is based on the expression of the *lacZ* gene which is under control of the *Hmox1* promoter. This promoter is predominantly induced by Nrf2, a transcription factor that is activated by ROS. 3-MCPD-mediated induction of *Hmox1* gene expression was confirmed by qRT-PCR in our study. Other Nrf2-dependent target genes were hardly affected in 3-MCPD-treated mice, especially in testes and brain (Fig. 5). Thus, our data do not support a general strong activation of the Nrf2 pathway by 3-MCPD. In contrast, 3-MCPD may trigger a more specific, possibly Nrf2-independent mechanism for the induction of *Hmox1* gene expression. Although Nrf2 has been shown to be the most important transcription factor for *Hmox1* promoter activation, binding sites for additional transcription factors such as heat-shock factor (HSF), nuclear factor-κB (NF-κB), and activating protein-1 (AP-1) have been identified in the Hmox1 promoter region. Thus, *Hmox1* gene transcription may be stimulated by hyperthermia (via HSF), inflammatory cytokines (via NF-kB) or specific phosphorylation-dependent signaling cascades (via AP-1). More specific functional studies, however, have revealed that the murine *Hmox1* promoter can be activated neither by HSF nor by NF-κB ((Alam and Cook 2007), and references herein). In contrast, AP-1 has been shown to stimulate murine *Hmox1* promoter activity (Elbirt et al. 1998; Gong et al. 2002). Thus, 3-MCPD-mediated *Hmox1* promoter activation might not necessarily be facilitated via Nrf2, but potentially via AP-1 instead. The exact molecular mechanism for 3-MCPD-triggered *Hmox1* promoter activation has to be elucidated in future studies.

Oxidation of the redox sensor protein DJ-1 was the most sensitive endpoint for 3-MCPD-induced oxidative stress response as irreversible oxidation of DJ-1 was observed in the medium dose group and in the low dose group of the present study (Fig. 6). It has been reported that oxidation of the redox-active cysteine residue of DJ-1 can be facilitated by hydrogen peroxide (Kinumi et al. 2004). Thus, it has been assumed that DJ-1 oxidation is mediated by ROS, however, the exact mechanism of DJ-1 oxidation is not known. The results of the present study does not support the notion that 3-MCPD-mediated DJ-1

oxidation is facilitated by ROS, because lipid peroxidation that was chosen as another endpoint to monitor ROS formation was not increased in the organs of 3-MCPD-treated mice. This observation leads to the conclusion that 3-MCPD does not induce general ROS formation. Thus, another more specific mechanism for DJ-1 oxidation seems to be triggered by 3-MCPD. Notably, 3-MCPD-induced DJ-1 oxidation in brain tissue has not been shown before. The results of the present study reveal that already moderate doses of 3-MCPD (1 mg/kg b.w./day in the present study) facilitate DJ-1 oxidation in mouse brain. Irreversible oxidation of DJ-1 is associated with the onset of a number of oxidative stress-related diseases such as Parkinson's disease (Ariga 2015; Wilson 2011). A few studies are available in which potential neurotoxic effects of 3-MCPD had been examined. Repeated doses of 100 mg 3-MCPD/kg b.w./day induced severe neurotoxic effects in mice such as hind-limb paralysis (Ford and Waites 1982), and led to severe morphological changes in the brain such as vacuolization and axonal degeneration of the sciatic nerve (Lee et al. 2015). On the other hand, no neurobehavioral deficits were observed in rats after repeated administration of 3-MCPD in doses of up to 30 mg/kg b.w./day over a period of 11 weeks (Kim et al. 2004). In that study, 3-MCPD treatment had no effect on the overall motor activity, on landing foot splay and on the fore limb grip strength of the animals, indicating that 3-MCPD does obviously not induce motoric deficits in rats that might be associated with 3-MCPD-mediated neurotoxic effects.

In conclusion, high repeated doses of 100 mg 3-MCPD/kg b.w./day induce severe oxidative stress in different 3-MCPD target organs of mice, finally leading to organ failure. 3-MCPD-mediated oxidative stress induced by doses in a range of 10 mg/kg b.w./day or below appears to be compensated by cellular ROS detoxification systems in all organs except for kidney. Thus, the finding that kidney is the most sensitive target organ of 3-MCPD toxicity was confirmed by the results of the present study. Regarding the molecular mechanism of 3-MCPD-mediated oxidative stress induction, our results indicate that 3-MCPD may trigger specific mechanism other than the Nrf2 pathway for an oxidative stress response. Oxidation of DJ-1 has been shown to be the most sensitive effect biomarker for 3-MCPD, however, the

well-documented link between DJ-1 oxidation and the onset of neurodegenerative diseases such as Parkinson's disease is questionable taking the results of (Kim et al. 2004) into account. Finally, it has to be noted that the oxidative stress-related effects observed in the present study only occurred by applying doses of 3-MCPD that are three to four orders of magnitude above reported human exposure levels, leading to the conclusion that 3-MCPD-mediated induction of oxidative stress may not be of relevance to deduce a concern for human health.

Acknowledgments

We thank Elke Zabinsky and Christine Meckert for helpful technical assistance. Tanya Frangova is thanked for help with animal work, and Cheryl Wood for tissue sectioning and staining. This project was funded by the German Federal Institute for Risk Assessment (project 1322-660). The HOTT mouse was developed under European Research Council Advanced Investigator Award number 294533.

Conflict of interest

The authors declare that they have no conflict of interest.

Ethical approval

All applicable international, national, and/or institutional guidelines for the care and use of animals were followed. All procedures performed in this study involving animals were in accordance with the ethical standards of the Animals Committee of the University of Dundee (permit number ND01/09/16).

Figure Legends

Figure 1 Mean body weights (a) and organ to body weight ratios (b) for male reporter mice treated with 3-MCPD. Mice received water (control), 1, 10 or 100 mg 3-MCPD/kg b.w./day for 28 days. The mice treated with 100 mg 3-MCPD/kg b.w./day had to be euthanized at day 7 due to severe weight loss (>20 %) and an overall bad constitution of all five animals. Data are given as mean + SD; n=4 for the control group and n=5 for the treatment groups; statistics by one-way ANOVA followed by Dunnett's multiple comparison test; * $p<0.05$; ** $p<0.01$; *** $p<0.001$

Figure 2 X-Gal staining of (a) kidney, (b) testes and (c) brain from HOTT reporter mice treated with water for 28 days (control) or with 100 mg 3-MCPD per kg b.w. for 7 days. Blue-colored areas indicate activation of the *Hmox1* promoter which is associated with oxidative stress response

Figure 3 Representative images of X-Gal-stained organ slices (a) and detailed microscopic images of the renal cortex (b) from HOTT reporter mice treated with water (control), 1, 10 and 100 mg 3-MCPD/kg b.w./day as indicated in the Figure

Figure 4 Densitometric evaluation of the microscopic images from the X-Gal-stained organ slices from HOTT reporter mice treated with water (control), 1, 10 and 100 mg 3-MCPD/kg b.w./day (see Figure 2 and 3). The blue-colored area was detected by using the ZEN lite blue edition software and set in relation to the total tissue area. Data evaluation was conducted for (a) kidney, (b) testes, (c) cerebellum, (d) midbrain and (e) pons. Data are expressed as mean + SD (n=4 for the control group, and n=5 for the treatment groups). Statistics, one-way ANOVA followed by Dunnett's multiple comparison test; * $p<0.05$; ** $p<0.01$; *** $p<0.001$

Figure 5 Gene expression analysis of genes associated with the Nrf2 pathway for ROS detoxification. Total mRNA was isolated from (a) kidney, (b) testes and (c) brain from HOTT reporter mice that had been treated with 0, 1, 10 or 100 mg 3-MCPD/kg b.w./day. Gene expression of glutathione S-transferase P1 (*Gstp1*), catalase (*Cat*), superoxide dismutase (*Sod1*), protein deglycase DJ-1 (*Park7*), endogenous heme oxygenase 1 (*Hmox1*), glutaredoxin (*Glrx1* and *Glrx2*), peroxiredoxin (*Prdx1* and *Prdx6*), sulfiredoxin 1 (*Srxn1*), glutathione reductase (*Gsr*), glutamate-cysteine ligase (*Gclc*) and glutathione synthetase (*Gss*) was conducted by qRT-PCR. Data were evaluated according to the ΔΔCt method by using β-actin as housekeeping gene and normalized against the expression values of the untreated control group. Statistics, one-way ANOVA followed by Dunnett's multiple comparison test; * $p<0.05$; ** $p<0.01$; *** $p<0.001$

Figure 6 Immunodetection of the DJ-1 protein by 2D-Western blotting analysis with protein extracts obtained from kidney, testes and brain from HOTT reporter mice that had been treated with 0, 1 or 10 mg 3-MCPD/kg b.w./day for 28 days. (a) Representative image obtained with a protein sample from mouse testes to illustrate the six different isoforms of DJ-1. (b) Representative 2D-Western blot images obtained from mouse kidney, testes and brain after treatment with water (control), 1 or 10 mg 3-MCPD/kg b.w./day. (c) Densitometric evaluation of the C and D spot intensities. Data are expressed as mean + SD (n=4 for the control group, and n=5 for the treatment groups). Statistics, one-way ANOVA followed by Dunnett's multiple comparison test; *** $p<0.001$

Figure 7 Immunodetection of 4-hydroxy-2-nonenal (4-HNE)-modified proteins. Protein extracts from (a) kidney, (b) testes and (c) brain from HOTT reporter mice treated with water (control; n=4) and 10 mg 3-MCPD/kg b.w./day (n=5) were subjected to SDS-PAGE and subsequent Western blot analysis by using an antibody raised against 4-HNE. (d) Densitometric evaluation of these Western blots. The sum of band intensities of an entire lane was normalized against the band intensity of GAPDH of the same lane. Moreover, data

were normalized against the values of the control groups that were set to 1 and expressed as mean + SD. Statistics, Student’s t-test; * $p < 0.05$

References

Abraham K, Appel KE, Berger-Preiss E, et al. (2013) Relative oral bioavailability of 3-MCPD from 3-MCPD fatty acid esters in rats. Archives of toxicology 87(4):649-59 doi:10.1007/s00204-012-0970-8

Alam J, Cook JL (2007) How many transcription factors does it take to turn on the heme oxygenase-1 gene? Am J Respir Cell Mol Biol 36(2):166-74 doi:10.1165/rcmb.2006-0340TR

Ariga H (2015) Common mechanisms of onset of cancer and neurodegenerative diseases. Biol Pharm Bull 38(6):795-808 doi:10.1248/bpb.b15-00125

Barocelli E, Conradi A, Mutti A, Petronini PG (2011) Comparison between 3-MCPD and its palmitic esters in a 90-day toxicological study. EFSA external scientific report, https://efsa.onlinelibrary.wiley.com/doi/epdf/10.2903/sp.efsa.2011.EN-187

Braeuning A, Sawada S, Oberemm A, Lampen A (2015) Analysis of 3-MCPD- and 3-MCPD dipalmitate-induced proteomic changes in rat liver. Food and chemical toxicology : an international journal published for the British Industrial Biological Research Association 86:374-84 doi:10.1016/j.fct.2015.11.010

Buhrke T, Schultrich K, Braeuning A, Lampen A (2017) Comparative analysis of transcriptomic responses to repeated-dose exposure to 2-MCPD and 3-MCPD in rat kidney, liver and testis. Food and chemical toxicology : an international journal published for the British Industrial Biological Research Association 106(Pt A):36-46 doi:10.1016/j.fct.2017.05.028

Buhrke T, Voss L, Briese A, et al. (2018) Oxidative inactivation of the endogenous antioxidant protein DJ-1 by the food contaminants 3-MCPD and 2-MCPD. Archives of toxicology 92(1):289-299 doi:10.1007/s00204-017-2027-5

Chen XL, Kunsch C (2004) Induction of cytoprotective genes through Nrf2/antioxidant response element pathway: a new therapeutic approach for the treatment of inflammatory diseases. Curr Pharm Des 10(8):879-91

Cho WS, Han BS, Nam KT, et al. (2008) Carcinogenicity study of 3-monochloropropane-1,2-diol in Sprague-Dawley rats. Food and chemical toxicology : an international journal published for the British Industrial Biological Research Association 46(9):3172-7 doi:10.1016/j.fct.2008.07.003

Craft BD, Chiodini A, Garst J, Granvogl M (2013) Fatty acid esters of monochloropropanediol (MCPD) and glycidol in refined edible oils. Food additives & contaminants Part A, Chemistry, analysis, control, exposure & risk assessment 30(1):46-51 doi:10.1080/19440049.2012.709196

EFSA (2016) Risks for human health related to the presence of 3- and 2-monochloropropanediol (MCPD), and their fatty acid esters, and glycidyl fatty acid esters in food. EFSA Journal 14(5):4426 doi:10.2903/j.efsa.2016.4426

EFSA (2018) Update of the risk assessment on 3-monochloropropane diol and its fatty acid esters. EFSA Journal 16(1):5083 doi:10.2903/j.efsa.2018.5083

Elbirt KK, Whitmarsh AJ, Davis RJ, Bonkovsky HL (1998) Mechanism of sodium arsenite-mediated induction of heme oxygenase-1 in hepatoma cells. Role of mitogen-activated protein kinases. J Biol Chem 273(15):8922-31

Ford WC, Waites GM (1982) Activities of various 6-chloro-6-deoxysugars and (S) alpha-chlorohydrin in producing spermatocoeles in rats and paralysis in mice and in inhibiting glucose metabolism in bull spermatozoa in vitro. J Reprod Fertil 65(1):177-83

Gong P, Stewart D, Hu B, Vinson C, Alam J (2002) Multiple basic-leucine zipper proteins regulate induction of the mouse heme oxygenase-1 gene by arsenite. Arch Biochem Biophys 405(2):265-74

IARC (2012) 3-Monochloro-1,2-propanediol IARC Monographs on the Evaluation of Carcinogenic Risks to Humans. IARC Press, Lyon, France 101:349-374
Jones AR, Milton DH, Murcott C (1978) The oxidative metabolism of alpha-chlorohydrin in the male rat and the formation of spermatocoeles. Xenobiotica 8(9):573-82 doi:10.3109/00498257809061257
Kim K, Song C, Park Y, et al. (2004) 3-monochloropropane-1,2-diol does not cause neurotoxicity in vitro or neurobehavioral deficits in rats. Neurotoxicology 25(3):377-85 doi:10.1016/j.neuro.2003.08.004
Kinumi T, Kimata J, Taira T, Ariga H, Niki E (2004) Cysteine-106 of DJ-1 is the most sensitive cysteine residue to hydrogen peroxide-mediated oxidation in vivo in human umbilical vein endothelial cells. Biochem Biophys Res Commun 317(3):722-8 doi:10.1016/j.bbrc.2004.03.110
Kuhlmann J (2011) Determination of bound 2,3-epoxy-1-propanol (glycidol) and bound monochloropropanediol (MCPD) in refined oils. Eur J Lipid Sci Tech 113(3):335-344 doi:DOI 10.1002/ejlt.201000313
Laemmli UK (1970) Cleavage of structural proteins during the assembly of the head of bacteriophage T4. Nature 227(5259):680-5
Lee BS, Park SJ, Kim YB, et al. (2015) A 28-day oral gavage toxicity study of 3-monochloropropane-1,2-diol (3-MCPD) in CB6F1-non-Tg rasH2 mice. Food and chemical toxicology : an international journal published for the British Industrial Biological Research Association 86:95-103 doi:10.1016/j.fct.2015.09.019
Luckert C, Ehlers A, Buhrke T, Seidel A, Lampen A, Hessel S (2013) Polycyclic aromatic hydrocarbons stimulate human CYP3A4 promoter activity via PXR. Toxicology letters 222(2):180-8 doi:10.1016/j.toxlet.2013.06.243
Luczaj W, Gegotek A, Skrzydlewska E (2017) Antioxidants and HNE in redox homeostasis. Free Radic Biol Med 111:87-101 doi:10.1016/j.freeradbiomed.2016.11.033
McMahon M, Ding S, Acosta-Jimenez LP, Frangova TG, Henderson CJ, Wolf CR (2018) Measuring in vivo responses to endogenous and exogenous oxidative stress using a novel haem oxygenase 1 reporter mouse. The Journal of physiology 596(1):105-127 doi:10.1113/jp274915
Sawada S, Oberemm A, Buhrke T, et al. (2015) Proteomic analysis of 3-MCPD and 3-MCPD dipalmitate toxicity in rat testis. Food and chemical toxicology : an international journal published for the British Industrial Biological Research Association 83:84-92 doi:10.1016/j.fct.2015.06.002
Sawada S, Oberemm A, Buhrke T, Merschenz J, Braeuning A, Lampen A (2016) Proteomic analysis of 3-MCPD and 3-MCPD dipalmitate-induced toxicity in rat kidney. Archives of toxicology 90(6):1437-48 doi:10.1007/s00204-015-1576-8
Scharmach E, Buhrke T, Lichtenstein D, Lampen A (2012) Perfluorooctanoic acid affects the activity of the hepatocyte nuclear factor 4 alpha (HNF4alpha). Toxicology letters 212(2):106-12 doi:10.1016/j.toxlet.2012.05.007
Wilson MA (2011) The role of cysteine oxidation in DJ-1 function and dysfunction. Antioxid Redox Signal 15(1):111-22 doi:10.1089/ars.2010.3481

Introduction

Fatty acid esters of 3-Chloro-1,2-propanediol (3-MCPD) are heat-induced food process contaminants that are predominantly formed during the refinement of vegetable oils and fats (Craft et al. 2013; Kuhlmann 2011). After ingestion with food, the esters are nearly quantitatively hydrolysed in the gastrointestinal tract, thereby liberating free 3-MCPD (Abraham et al. 2013; Barocelli et al. 2011). The free compound is readily resorbed into the body and partially excreted with the urine. 3-MCPD is metabolized i) to its oxidation product β-chlorolactic acid and ii) to dihydroxypropylmercapturic acid (DHPMA) which is the terminal product of an initial 3-MCPD glutathione conjugate. As for non-modified 3-MCPD, both metabolites are also excreted with urine (Barocelli et al. 2011; Jones et al. 1978).

3-MCPD has been classified to be non-genotoxic and possibly carcinogenic to humans (category 2B; (IARC 2012). In long-term feeding studies, repeated oral application of 3-MCPD at doses as low as 2 mg/kg b.w./day caused nephrotoxicity (tubular hyperplasia), testicular toxicity (atrophy and arteritis) in male rats, and nephrotoxicity in female rats. Moreover, an increased incidence for Leydig cell tumors and kidney tubular adenoma were observed (Cho et al. 2008). The underlying molecular mechanisms that are associated with the carcinogenic potential of 3-MCPD, however, are barely known. To unravel the molecular toxicity mechanism(s) of 3-MCPD, a 28-day feeding study with rats was conducted followed by the analysis of proteomic and transcriptomic alterations induced by 3-MCPD in different rat organs. Bioinformatic evaluation of these proteomic and transcriptomic data revealed that 3-MCPD induced oxidative stress and affected glutathione metabolism in rat kidney and testes and inhibited glycolysis in rat testes (Buhrke et al. 2017; Sawada et al. 2015; Sawada et al. 2016). In a more detailed analysis, the redox sensor protein DJ-1 was identified to be a sensitive biomarker for 3-MCPD-mediated oxidative stress (Buhrke et al. 2018).

In the present study, so-called HOTT reporter mice were employed to study the impact of 3-MCPD on oxidative stress response *in vivo* in more detail. In the transgenic HOTT mice, the bacterial *lacZ* gene encoding β-galactosidase is under the control of the heme oxygenase 1

(*Hmox1*) promoter. The *Hmox1* promoter is activated by pro-oxidant stimuli, predominantly via the Nrf2 transcription factor. Oxidative stress-mediated *Hmox1* promoter activation induces *lacZ* gene expression. β-galactosidase activity can then easily be visualized by using the common X-Gal staining, and blue-colored regions in X-Gal-stained organ slices indicate a high burden of oxidative stress in these regions (McMahon et al. 2018). Thus, the use of HOTT reporter mice in the present study was a straight-forward approach to identify the organs that were affected by 3-MCPD-mediated oxidative stress and to study the oxidative stress response in these organs in detail.

Materials and Methods

Animal study

The animal work in this study was carried out under the Animals (Scientific Procedures) act (1986) and EU Directive 2010/63/EU after approval by the Welfare and Ethical treatment of Animals Committee of the University of Dundee and the University Veterinary Surgeon. The heterozygous heme oxygenase triple transgenic (HOTT) reporter mice on a C57BL/6NTac background were supplied by the Medical School Resource Unit, University of Dundee (McMahon et al. 2018).

20 young adult (16-20 weeks, n=5) male mice, weighting ~ 25 g, were randomly allocated to four groups. Group 1 served as vehicle control and was treated with water by oral gavage, daily for 28 days. Animals of groups 2, 3 and 4 received 1, 10 and 100 mg 3-MCPD (Sigma-Aldrich, Munich, Germany) per kg body weight for 28 days, respectively, by oral gavage.

Animals were housed in open-top cages with *ad libitum* access to food (RM1, Special Diet Services, Essex, UK) and water. Mice were held at 12 h light/dark environment with temperature between 20 - 24°C and relative humidity between 45 - 65%.

Animals were euthanized by a rising concentration of CO_2 and death was confirmed by exsanguination. Kidney, testes, brain, liver, heart and spleen were harvested, individually weighed and cut. Half a medium lobe of the liver was fixed in 10 % neutral buffered formalin and the other half in 1 % paraformaldehyde. For all other organs, one half was snap-frozen and stored at -80°C, and the second half was fixed with Mirsky's fixative (National Diagnostics, Atlanta, USA) overnight at 4°C, and afterwards all tissues were washed in PBS containing 2 mM $MgCl_2$, dehydrated in 30 % sucrose and embedded in Shandon M-1 Embedding Matrix (Thermo Fisher Scientific, Waltham, USA) in a dry ice–isopentane bath. The organs were cut at 10 µm thickness on an OFT5000 cryostat (Bright Instrument Co., Luton, UK) at -20°C.

Organs from Group 4 mice were removed post mortem, rinsed in ice-old sterile PBS and fixed in 4% (w/v) formaldehyde (Gurr; VWR, UK) overnight before being transferred into 70%

(v/v) ethanol. The next day, tissues were dehydrated (Shandon Citadel 1000, Thermo Scientific, UK), and embedded in paraffin wax (Shandon Histocentre 3, Thermo Scientific, UK).

Histochemical analysis

LacZ staining

Slides with 10 µm tissue slices were placed in a staining tray and allowed to equilibrate to room temperature, and then rehydrated in PBS supplemented with 2 mM $MgCl_2$ for 5 min. The slices were entirely covered with X-Gal staining solution (PBS (pH 7.4) including 2 mM $MgCl_2$, 0.01% (w/v) sodium deoxycholate, 0.02% (v/v) Igepal CA630, 5 mM potassium ferricyanide, 5 mM potassium ferrocyanide and 1 mg/ml X-Gal [5-bromo-4-chloro-3-indolyl β-D-galactopyranoside]) and incubated in a humidified chamber at 37°C overnight. The next day, slides were washed with PBS and counterstained with Nuclear Fast Red (Vector Laboratories, Burlingame, USA). Subsequently, organ slices were washed twice with double-distilled water and dehydrated with 70 % ethanol followed by 95 % ethanol and incubated in Histoclear (VWR, Radnor, USA) for 3 min. After air-drying, coverslips were applied by using DPX mountant (Sigma-Aldrich, Munich, Germany).

Densitometric evaluation

The software ZEN 2.3 lite blue edition (Carl Zeiss Microscopy, Thornwood, USA) was used for quantitative image analysis of the X-Gal staining. The densitometric analysis was based on microscope images which were acquired with a Zeiss Axio Observer (Carl Zeiss, Jena, Germany). The images were analyzed by using a customized automatic segmentation algorithm for each image. For the automatic segmentation a threshold for the red, green and blue (RGB) channels was defined in order to filter the area of blue coloration within the image. The value of each RGB channel of each pixel had to be below the threshold to remove the background in each image and to quantify the corresponding pixels as X-Gal positive. For image analysis, the following segmentation parameters were used: smooth:

none; sharpen: none; minimum area: 1; threshold: red 0-1468, green 0-1366, blue 0-1839; tolerance: 3 %; neighborhood: 1; separate: morphology; count: 3. After the software automatically determined the area of blue coloration within the microscopic image, the total area of the image was set in relation to the area of the measured blue staining. Subsequently, the percentage of the area of X-Gal positive staining of each acquired microscope image was determined. For the kidney cortex and testes, five images were analyzed for each animal whereas three images were analyzed for midbrain, cerebellum and pons for each animal.

Protein extraction and Western blotting

For protein extraction, 50-60 mg of frozen tissue from mouse kidney, testes or brain was disrupted in the presence of liquid nitrogen by using mortar and pestle. The frozen tissue powder was suspended in lysis buffer (50 mM Tris-HCl (pH 7.5), 150 mM NaCl, 2 µM EGTA, 0.1 % (w/v) SDS, 0.5 % (w/v) deoxycholic acid, 2 % complete protease inhibitor cocktail 1x (Roche, Basel, Switzerland)) and further homogenized by stepwise sonification. The protein extract were centrifuged at 20,000 x g for 30 min at 4°C, and the supernatant was stored at −80 °C. The protein content was determined by using the Bicinchoninic Acid Kit for Protein Determination (Sigma-Aldrich, Munich, Germany).

2DE Western blotting

2D gel electrophoresis was performed according to (Buhrke et al. 2018) with the modification that the Ettan IPGphor IEF separation unit (GE Healthcare, Freiburg, Germany) was used as follows: 300 V for 1 h, gradient from 300 to 1000 V within 1 h, gradient from 1000 to 5000 V within 2 h, and finally 5000 V for 1.5 h. The polyacrylamide gel electrophoresis was conducted according to the protocol of (Laemmli 1970) by using a 12 % polyacrylamide gel.

2D gels were blotted according to (Scharmach et al. 2012) by using a rabbit monoclonal antibody raised against PARK7/DJ1 (ab76008; Abcam, Cambridge, UK) in 1:5000 dilution, and goat-anti-rabbit-IgG-HRP (HAF008, R&D systems, Minneapolis, Canada) in a 1:2000

dilution as secondary antibody. For acquisition of the chemiluminescent Western blot a VersaDoc MP4000 Imaging System was used (Bio-Rad, Munich, Germany).

Densitometric analysis of the spot intensities from the 2D-Western blots was carried out by using the Image Lab 5.2 software (Bio-Rad, Munich, Germany). Spot intensities were compared to the intensities of the other spots on the same blot and expressed as relative intensities.

1D Western blotting

1D Western blotting for detection of 4-HNE protein adducts was carried out and detected as described above (Laemmli 1970; Scharmach et al. 2012). 20 µg of protein per lane and a 12 % polyacrylamide gel was used for the electrophoretic separation. The Western blotting was conducted by using rabbit polyclonal antibody against 4-HNE (ab46545, Abcam, Cambridge, UK) in a 1:1000 dilution and a goat-anti-rabbit-IgG-HRP (HAF008, R&D systems, Minneapolis, Canada) in a 1:5000 dilution as secondary antibody. For restaining of glyceraldehyde-3-phosphate dehydrogenase (GAPDH) as loading control, the primary and secondary antibodies of 4-HNE detection were removed from the blot membrane by incubating the membrane for 30 minutes at 55°C in stripping solution pH 6.7 (62 mM Tris-HCl, 5 % SDS and 0.88 % β-mercaptoethanol) with agitation. After washing the membrane with TBST for 10 minutes the restain of GAPDH was carried out using mouse monoclonal antibody against GAPDH (ab8245, Abcam, Cambridge, UK) in a 1:7500 dilution and a secondary goat-anti-mouse-IgG-HRP antibody (A-014HRP, Seramun Diagnostica, Heidesee, Germany) in a 1:10000 dilution. Detection and densitometric analysis was carried out as described above. Single band intensities were compared to the intensities of the entire lane and expressed as relative intensities in relation to GAPDH.

RNA isolation and quantitative real-time RT-PCR

Total mRNA was extracted from all animals of Group 1, 2 and 3. After disruption of 15-30 mg frozen tissue by a mortar and pestle in liquid nitrogen, the RNA was homogenized and

isolated by using the RNeasy Mini Kit (Qiagen, Hilden, Germany). The organs from Group 4 were formalin-fixed and paraffin-embedded. The extraction of total mRNA from these tissues was done by using the RNeasy FFPE Kit (Qiagen, Hilden, Germany). The concentration of RNA was determined with a NanoDrop ND-1000 spectrometer (NanoDrop Technologies, Wilmington, DE, USA).

The isolated mRNA samples were reverse transcribed by using the high capacity cDNA reverse transcription kit (Applied Biosystem/ Life Technologies GmbH, Darmstadt, Germany). Afterwards, the cDNA was subjected to PCR analysis via Maxima SYBR Green/Rox qPCR Master Mix (Thermo Fisher Scietific, Waltham, MA, USA) and a Stratagene MX3005P real-time PCR cycler according to the protocol by (Luckert et al. 2013). Gene expression was calculated by relative quantification according to the ΔΔCt method and normalization with β-actin as reference gene.

The following primer were used: β-Actin 5'-GATCATTGCTCCTCCTGAGC-3' (forward) and 5'-CATCGTACTCCTGCTTGCTG-3', glutathione S-transferase P1 (*Gstp1*) 5'-ATATGTCACCCTCATCTACACCA-3' (forward) and 5'-CTGGTCACCCACGATGAAAG-3' (reverse), catalase (*Cat*) 5'-CAATGGCAATTACCCGTCCTG-3' (forward) and 5'-TAGTCCTTGTGAGGCCAAACC-3' (reverse), superoxide dismutase 1 (*Sod1*) 5'-GGGTTCCACGTCCATCAGTAT-3' (forward) and 5'-CCTTTCCAGCAGTCACATTGC-3' (reverse), protein deglycase (*Park7*) 5'- GCTCTGTTGGCTCACGAAGT-3' (forward) and 5'TCCTTAGCCAGTGGGTGTGT-3' (reverse), heme oxygenase 1 (*Hmox1*) 5'-GCAGAACCCAGTCTATGCCC-3' (forward) and 5'- GGCGTGCAAGGGATGATTTC-3' (reverse), glutaredoxin 1 (*Glrx1*) 5'-CTCACCGGAGCGAGAACAG-3' (forward) and 5'-TCTGCTTCAGCCGAGTCATC-3' (reverse), glutaredoxin 2 (*Glrx2*) 5'-ACAAGGCTGTGGAGTTGGAT-3' (forward) and 5'-GCTGCGCCTCCAATAAATCG-3' (reverse), peroxiredoxin 1 (*Prdx1*) 5'-AGTGATTGGCGCTTCTGTGG-3' (forward) and 5'-AATGGTGCGCTTGGGATCTG-3' (reverse), peroxiredoxin 6 (*Prdx6*) 5'-CAGGGACCTTGCCATCCTTT-3' (forward) and 5'-AGGCATGTTGTTAGCGTCCT-3' (reverse), sulfiredoxin 1 (*Srxn1*) 5'-TACCAATCGCCGTGCTCATC-3' (forward) and 5'-

AGTAGTAGTCGCCACCCTGG-3’ (reverse), glutathione reductase (*Gsr*) 5’-CGAGGAACTGGAGAATGCCG-3’ (forward) and 5’-TCTGGAATCATGGTCGTGGTG-3’ (reverse), glutamate-cysteine ligase catalytic subunit (*Gclc*) 5’-TGACATCGACCTGACCATCG-3’ (forward) and 5’-AACGTGCTGTGCCAGAAGAT-3’ (reverse), glutathione synthetase (*Gss*) 5’-ATGCGGTGGTGCTACTGATT-3’ (forward) and 5’-TACGGCACGCTGGTCAAATA-3’ (reverse).

Statistics

Statistical analysis was carried out using the One Way Analysis of Variance (ANOVA) followed by Dunnett’s multiple comparison tests. Statistical significance was assumed at $p<0.05$.

Results

To examine which organs are predominantly affected by 3-MCPD-induced oxidative stress, HOTT reporter mice were daily treated with 3-MCPD for 28 days. One animal of the control group (Group 1) was found dead at day 7, and the organs of this mouse were not preserved for further analysis. Thus, the control group consisted of four animals whereas the three treatment groups consisted of five animals each. The mice of the high dose group (100 mg 3-MCPD/kg b.w./day; Group 4) had to be euthanized at day 7 due to severe weight loss (> 20%) and an overall bad constitution of all five animals. Thus, it has to be noted that all results regarding the high dose group have been obtained from mice showing signs of acute toxicity at sacrifice after 7 days of 3-MCPD treatment, whereas the animals of the other groups showed no clinical symptoms or signs of acute toxicity and were sacrificed after 28 days of 3-MCPD treatment. Following the animal weights, the mice of the low and the medium dose groups displayed weight curves within the treatment period of 28 days comparable to the mice of the control group whereas the mice of the high dose group lost weight until they had to be euthanized at day 7 (Fig. 1a). No gross phenotypic anomalies were recorded. Regarding the organ to body weight ratios, increased relative weights were observed for kidney, brain and heart of the animals of the high dose group and for the hearts of the animals of the medium dose group. The organ to body weight ratios of other organs were not affected upon 3-MCPD treatment (Fig. 1b).

Microscopic slices were prepared from different organs of the HOTT mice and subjected to X-Gal staining. Strong blue stain was observed for the entire kidney cortex from the mice of the high dose group compared to the control group (Fig. 2a). As the *lacZ* gene in the HOTT reporter mice is under the control of the ROS-sensitive *Hmox1* promoter, blue-colored regions are indicative for a high ROS burden in the respective organ (McMahon et al. 2018). Thus, the animals of the high dose group were suffering from severe oxidative stress in their kidneys. Moreover, the X-Gal staining was more intense in the seminiferous tubules of the testes of the mice from the high dose group compared to the control group (Fig. 2b). Finally,

specific regions of the brains of the mice from the high dose group, namely cerebellum, midbrain and pons, were clearly stained blue whereas there was almost no stain visible in the brains of the control mice (Fig. 2c). Compared to these strong effects in the organs from the mice of the high dose group, the effects observed in the organs from the animals of the low dose and medium dose groups were more moderate (Fig. 3a). Indeed, densitometric evaluation of the X-Gal staining revealed that a statistically significant dose-dependent increase of the blue color was only observed for the kidney (Fig. 4a). With respect to testes and brain, a significant increase of X-Gal-positive cells was only observed for the animals from the high dose group (Fig. 4b-e). In contrast to kidneys, testes and brain, no dose-dependent increase of the X-Gal staining was visible in liver, heart and spleen (data not shown). Regarding X-Gal staining in kidney cortex, a more detailed inspection revealed that blue stain first appeared in the glomeruli whereas kidney tubules were stained only at higher 3-MCPD doses (Fig. 3b).

To evaluate a potential oxidative stress response in the different mouse organs at the molecular level, the impact of 3-MCPD on gene expression of a number of Nrf2-dependent genes was examined. Nrf2 is a transcription factor that is activated under oxidative stress conditions and that promotes gene expression of a number of genes whose products have a function in ROS detoxification (Chen and Kunsch 2004). Gene expression of *Gstp1*, *Cat*, *Sod1*, *Park7*, *Hmox1*, *Glrx2*, *Prdx1*, *Prdx6*, *Gclc* and *Gss* was only slightly stimulated by 3-MCPD in mouse kidney with the strongest effects being observed for the high dose group. Notably, *Sod1*, *Glrx2* and *Gss* gene expression was significantly decreased in the kidneys of the mice from the high dose group (Fig. 5a). In mouse testes and brain, 3-MCPD hardly affected gene expression of the Nrf2-dependent genes examined in this study (Fig. 5b-c). A significant induction was only observed for *Gss* in testes and brain and for *Hmox1* in the brains of the animals from the high dose group, however, gene expression of *Gstp1*, *Sod1*, *Glrx1*, *Glrx2*, *Prdx1*, *Srxn1* and *Gsr* was significantly downregulated in testes and brain from the animals of the high dose group. Taken together, there was no strong and no clear dose-

dependent effect of 3-MCPD on the expression of several genes associated with the Nrf2 pathway in mouse kidney, testes and brain.

In a previous study, oxidation of the redox sensor protein DJ-1 (Park7) was shown to be a sensitive biomarker for 3-MCPD-induced oxidative stress in different rat organs (Buhrke et al. 2018). The irreversible oxidation of a redox-sensitive cysteine residue in DJ-1 to a sulfonic acid under oxidative stress conditions can be monitored by 2D-Western blot experiments. Thus, protein samples from different mouse organs from the present study were subjected to two-dimensional gel electrophoresis, and DJ-1 oxidation was evaluated by 2D-Western blotting. At least six different DJ-1 immunoreactive protein spots (labelled A to F) with spots C and D being the most intense ones have been detected (Fig. 6a). According to the results of the previous study, it can be assumed that spot D represents the non-modified DJ-1 protein with the redox-sensitive cysteine residue in its reduced thiol form whereas spot C represents DJ-1 with a cysteine residue being fully oxidized to a sulfonic acid (Buhrke et al. 2018). Representative 2D-Western blot images obtained with protein samples from mouse kidney, testes and brain are shown in Fig. 6b. Densitometric evaluation of the 2D-Western blot images revealed a significant decrease of the reduced DJ-1 form (spot D) accompanied by a significant increase of the oxidized DJ-1 form (spot C) in kidney, testes and brain of the animals from the low dose and the medium dose groups compared to those from the control group (Fig. 6c). Thus, treatment of the HOTT reporter mice with 3-MCPD led to an irreversible oxidation of the DJ-1 protein. *Park7* gene expression, on the other hand, was hardly affected in mouse kidney and not altered in testes and brain upon 3-MCPD treatment (Fig. 5).

Lipid peroxidation was chosen as an additional endpoint to monitor the oxidative stress response in the different mouse organs. For this purpose, protein samples from these organs were separated by SDS-PAGE and subjected to Western blot analysis by using an antibody raised against protein adducts of 4-hydroxynonenal (4-HNE). These adducts indicate the presence of 4-HNE which is a lipid peroxidation product that is formed in the presence of ROS (Luczaj et al. 2017). 4-HNE-protein adducts were detected in the protein samples

obtained from kidney, testes and brain from all animals from the control group and from the medium dose group (Fig. 7a-c). Densitometric evaluation of the band intensities of these blots revealed that the amount of 4-HNE-protein adducts was not altered in these mouse organs upon 3-MCPD treatment (Fig. 7d). Thus, 3-MCPD treatment did not result in an increase of lipid peroxidation in mouse kidney, testes and brain.

Discussion

The food contaminant 3-MCPD is classified as a non-genotoxic carcinogen with kidney and testes being the main target organs according to the results of different animal studies (EFSA 2016; EFSA 2018). In the past few years, we have conducted a number a proteomic and transcriptomic studies to elucidate the underlying molecular mechanism(s) that are associated with the carcinogenic potential of 3-MCPD. The results of these omics screening approaches pointed to a 3-MCPD-mediated induction of oxidative stress accompanied by a deregulation of glutathione metabolism in rat kidney, testes and liver (Braeuning et al. 2015; Buhrke et al. 2017; Sawada et al. 2015; Sawada et al. 2016). In a more detailed analysis, the redox sensor protein DJ-1 was identified to be irreversibly oxidized in different rat organs when 3-MCPD was administered to the animals (Buhrke et al. 2018). Loss of function of DJ-1 by irreversible oxidation is associated with a number of oxidative stress-related diseases such as Parkinson's disease (Ariga 2015; Wilson 2011), thus, putting the brain also into the focus of our 3-MCPD research in addition to the well-known target organs kidney and testes.

In the present study, we took advantage of the HOTT reporter mice that allow an easy visualization and quantification of oxidative stress responses in various mouse organs. After 3-MCPD administration, clear responses in kidney, testes and brain were observed (Fig. 3) whereas there was no increase in X-Gal-derived blue stain in liver and spleen (data not shown). Strong effects, however, were only observed for the animals of the high dose group. These animals had to be sacrificed after seven days of 3-MCPD administration as they had lost > 20% body weight and showed an overall bad constitution. Thus, 3-MCPD-mediated induction of oxidative stress seems, in most organs, to correlate with acute toxicity rather than with long-term exposure to low doses of the compound. In this context, it has to be noted that the doses of 3-MCPD used in the present study are three to four orders of magnitude above human exposure levels, i.e. the doses consumers regularly ingest with food. The tolerable daily intake was recently set to 2 µg/kg b.w./day, and it was stated that for the general population it is unlikely that this TDI is exceeded (EFSA 2018). Thus, it is

questionable whether oxidative stress responses induced by high doses of 3-MCPD as observed in this study are relevant for human health at normal dietary exposure.

X-Gal staining of tissue slices from HOTT mice is based on the expression of the *lacZ* gene which is under control of the *Hmox1* promoter. This promoter is predominantly induced by Nrf2, a transcription factor that is activated by ROS. 3-MCPD-mediated induction of *Hmox1* gene expression was confirmed by qRT-PCR in our study. Other Nrf2-dependent target genes were hardly affected in 3-MCPD-treated mice, especially in testes and brain (Fig. 5). Thus, our data do not support a general strong activation of the Nrf2 pathway by 3-MCPD. In contrast, 3-MCPD may trigger a more specific, possibly Nrf2-independent mechanism for the induction of *Hmox1* gene expression. Although Nrf2 has been shown to be the most important transcription factor for *Hmox1* promoter activation, binding sites for additional transcription factors such as heat-shock factor (HSF), nuclear factor-κB (NF-κB), and activating protein-1 (AP-1) have been identified in the Hmox1 promoter region. Thus, *Hmox1* gene transcription may be stimulated by hyperthermia (via HSF), inflammatory cytokines (via NF-kB) or specific phosphorylation-dependent signaling cascades (via AP-1). More specific functional studies, however, have revealed that the murine *Hmox1* promoter can be activated neither by HSF nor by NF-κB ((Alam and Cook 2007), and references herein). In contrast, AP-1 has been shown to stimulate murine *Hmox1* promoter activity (Elbirt et al. 1998; Gong et al. 2002). Thus, 3-MCPD-mediated *Hmox1* promoter activation might not necessarily be facilitated via Nrf2, but potentially via AP-1 instead. The exact molecular mechanism for 3-MCPD-triggered *Hmox1* promoter activation has to be elucidated in future studies.

Oxidation of the redox sensor protein DJ-1 was the most sensitive endpoint for 3-MCPD-induced oxidative stress response as irreversible oxidation of DJ-1 was observed in the medium dose group and in the low dose group of the present study (Fig. 6). It has been reported that oxidation of the redox-active cysteine residue of DJ-1 can be facilitated by hydrogen peroxide (Kinumi et al. 2004). Thus, it has been assumed that DJ-1 oxidation is mediated by ROS, however, the exact mechanism of DJ-1 oxidation is not known. The results of the present study does not support the notion that 3-MCPD-mediated DJ-1

oxidation is facilitated by ROS, because lipid peroxidation that was chosen as another endpoint to monitor ROS formation was not increased in the organs of 3-MCPD-treated mice. This observation leads to the conclusion that 3-MCPD does not induce general ROS formation. Thus, another more specific mechanism for DJ-1 oxidation seems to be triggered by 3-MCPD. Notably, 3-MCPD-induced DJ-1 oxidation in brain tissue has not been shown before. The results of the present study reveal that already moderate doses of 3-MCPD (1 mg/kg b.w./day in the present study) facilitate DJ-1 oxidation in mouse brain. Irreversible oxidation of DJ-1 is associated with the onset of a number of oxidative stress-related diseases such as Parkinson's disease (Ariga 2015; Wilson 2011). A few studies are available in which potential neurotoxic effects of 3-MCPD had been examined. Repeated doses of 100 mg 3-MCPD/kg b.w./day induced severe neurotoxic effects in mice such as hind-limb paralysis (Ford and Waites 1982), and led to severe morphological changes in the brain such as vacuolization and axonal degeneration of the sciatic nerve (Lee et al. 2015). On the other hand, no neurobehavioral deficits were observed in rats after repeated administration of 3-MCPD in doses of up to 30 mg/kg b.w./day over a period of 11 weeks (Kim et al. 2004). In that study, 3-MCPD treatment had no effect on the overall motor activity, on landing foot splay and on the fore limb grip strength of the animals, indicating that 3-MCPD does obviously not induce motoric deficits in rats that might be associated with 3-MCPD-mediated neurotoxic effects.

In conclusion, high repeated doses of 100 mg 3-MCPD/kg b.w./day induce severe oxidative stress in different 3-MCPD target organs of mice, finally leading to organ failure. 3-MCPD-mediated oxidative stress induced by doses in a range of 10 mg/kg b.w./day or below appears to be compensated by cellular ROS detoxification systems in all organs except for kidney. Thus, the finding that kidney is the most sensitive target organ of 3-MCPD toxicity was confirmed by the results of the present study. Regarding the molecular mechanism of 3-MCPD-mediated oxidative stress induction, our results indicate that 3-MCPD may trigger specific mechanism other than the Nrf2 pathway for an oxidative stress response. Oxidation of DJ-1 has been shown to be the most sensitive effect biomarker for 3-MCPD, however, the

well-documented link between DJ-1 oxidation and the onset of neurodegenerative diseases such as Parkinson's disease is questionable taking the results of (Kim et al. 2004) into account. Finally, it has to be noted that the oxidative stress-related effects observed in the present study only occurred by applying doses of 3-MCPD that are three to four orders of magnitude above reported human exposure levels, leading to the conclusion that 3-MCPD-mediated induction of oxidative stress may not be of relevance to deduce a concern for human health.

Acknowledgments

We thank Elke Zabinsky and Christine Meckert for helpful technical assistance. Tanya Frangova is thanked for help with animal work, and Cheryl Wood for tissue sectioning and staining. This project was funded by the German Federal Institute for Risk Assessment (project 1322-660). The HOTT mouse was developed under European Research Council Advanced Investigator Award number 294533.

Conflict of interest

The authors declare that they have no conflict of interest.

Ethical approval

All applicable international, national, and/or institutional guidelines for the care and use of animals were followed. All procedures performed in this study involving animals were in accordance with the ethical standards of the Animals Committee of the University of Dundee (permit number ND01/09/16).

Figure Legends

Figure 1 Mean body weights (a) and organ to body weight ratios (b) for male reporter mice treated with 3-MCPD. Mice received water (control), 1, 10 or 100 mg 3-MCPD/kg b.w./day for 28 days. The mice treated with 100 mg 3-MCPD/kg b.w./day had to be euthanized at day 7 due to severe weight loss (>20 %) and an overall bad constitution of all five animals. Data are given as mean + SD; n=4 for the control group and n=5 for the treatment groups; statistics by one-way ANOVA followed by Dunnett's multiple comparison test; * $p<0.05$; ** $p<0.01$; *** $p<0.001$

Figure 2 X-Gal staining of (a) kidney, (b) testes and (c) brain from HOTT reporter mice treated with water for 28 days (control) or with 100 mg 3-MCPD per kg b.w. for 7 days. Blue-colored areas indicate activation of the *Hmox1* promoter which is associated with oxidative stress response

Figure 3 Representative images of X-Gal-stained organ slices (a) and detailed microscopic images of the renal cortex (b) from HOTT reporter mice treated with water (control), 1, 10 and 100 mg 3-MCPD/kg b.w./day as indicated in the Figure

Figure 4 Densitometric evaluation of the microscopic images from the X-Gal-stained organ slices from HOTT reporter mice treated with water (control), 1, 10 and 100 mg 3-MCPD/kg b.w./day (see Figure 2 and 3). The blue-colored area was detected by using the ZEN lite blue edition software and set in relation to the total tissue area. Data evaluation was conducted for (a) kidney, (b) testes, (c) cerebellum, (d) midbrain and (e) pons. Data are expressed as mean + SD (n=4 for the control group, and n=5 for the treatment groups). Statistics, one-way ANOVA followed by Dunnett's multiple comparison test; * $p<0.05$; ** $p<0.01$; *** $p<0.001$

Figure 5 Gene expression analysis of genes associated with the Nrf2 pathway for ROS detoxification. Total mRNA was isolated from (a) kidney, (b) testes and (c) brain from HOTT reporter mice that had been treated with 0, 1, 10 or 100 mg 3-MCPD/kg b.w./day. Gene expression of glutathione S-transferase P1 (*Gstp1*), catalase (*Cat*), superoxide dismutase (*Sod1*), protein deglycase DJ-1 (*Park7*), endogenous heme oxygenase 1 (*Hmox1*), glutaredoxin (*Glrx1* and *Glrx2*), peroxiredoxin (*Prdx1* and *Prdx6*), sulfiredoxin 1 (*Srxn1*), glutathione reductase (*Gsr*), glutamate-cysteine ligase (*Gclc*) and glutathione synthetase (*Gss*) was conducted by qRT-PCR. Data were evaluated according to the ΔΔCt method by using β-actin as housekeeping gene and normalized against the expression values of the untreated control group. Statistics, one-way ANOVA followed by Dunnett's multiple comparison test; * $p<0.05$; ** $p<0.01$; *** $p<0.001$

Figure 6 Immunodetection of the DJ-1 protein by 2D-Western blotting analysis with protein extracts obtained from kidney, testes and brain from HOTT reporter mice that had been treated with 0, 1 or 10 mg 3-MCPD/kg b.w./day for 28 days. (a) Representative image obtained with a protein sample from mouse testes to illustrate the six different isoforms of DJ-1. (b) Representative 2D-Western blot images obtained from mouse kidney, testes and brain after treatment with water (control), 1 or 10 mg 3-MCPD/kg b.w./day. (c) Densitometric evaluation of the C and D spot intensities. Data are expressed as mean + SD (n=4 for the control group, and n=5 for the treatment groups). Statistics, one-way ANOVA followed by Dunnett's multiple comparison test; *** $p<0.001$

Figure 7 Immunodetection of 4-hydroxy-2-nonenal (4-HNE)-modified proteins. Protein extracts from (a) kidney, (b) testes and (c) brain from HOTT reporter mice treated with water (control; n=4) and 10 mg 3-MCPD/kg b.w./day (n=5) were subjected to SDS-PAGE and subsequent Western blot analysis by using an antibody raised against 4-HNE. (d) Densitometric evaluation of these Western blots. The sum of band intensities of an entire lane was normalized against the band intensity of GAPDH of the same lane. Moreover, data

were normalized against the values of the control groups that were set to 1 and expressed as mean + SD. Statistics, Student’s t-test; * $p < 0.05$

References

Abraham K, Appel KE, Berger-Preiss E, et al. (2013) Relative oral bioavailability of 3-MCPD from 3-MCPD fatty acid esters in rats. Archives of toxicology 87(4):649-59 doi:10.1007/s00204-012-0970-8

Alam J, Cook JL (2007) How many transcription factors does it take to turn on the heme oxygenase-1 gene? Am J Respir Cell Mol Biol 36(2):166-74 doi:10.1165/rcmb.2006-0340TR

Ariga H (2015) Common mechanisms of onset of cancer and neurodegenerative diseases. Biol Pharm Bull 38(6):795-808 doi:10.1248/bpb.b15-00125

Barocelli E, Conradi A, Mutti A, Petronini PG (2011) Comparison between 3-MCPD and its palmitic esters in a 90-day toxicological study. EFSA external scientific report, https://efsa.onlinelibrary.wiley.com/doi/epdf/10.2903/sp.efsa.2011.EN-187

Braeuning A, Sawada S, Oberemm A, Lampen A (2015) Analysis of 3-MCPD- and 3-MCPD dipalmitate-induced proteomic changes in rat liver. Food and chemical toxicology : an international journal published for the British Industrial Biological Research Association 86:374-84 doi:10.1016/j.fct.2015.11.010

Buhrke T, Schultrich K, Braeuning A, Lampen A (2017) Comparative analysis of transcriptomic responses to repeated-dose exposure to 2-MCPD and 3-MCPD in rat kidney, liver and testis. Food and chemical toxicology : an international journal published for the British Industrial Biological Research Association 106(Pt A):36-46 doi:10.1016/j.fct.2017.05.028

Buhrke T, Voss L, Briese A, et al. (2018) Oxidative inactivation of the endogenous antioxidant protein DJ-1 by the food contaminants 3-MCPD and 2-MCPD. Archives of toxicology 92(1):289-299 doi:10.1007/s00204-017-2027-5

Chen XL, Kunsch C (2004) Induction of cytoprotective genes through Nrf2/antioxidant response element pathway: a new therapeutic approach for the treatment of inflammatory diseases. Curr Pharm Des 10(8):879-91

Cho WS, Han BS, Nam KT, et al. (2008) Carcinogenicity study of 3-monochloropropane-1,2-diol in Sprague-Dawley rats. Food and chemical toxicology : an international journal published for the British Industrial Biological Research Association 46(9):3172-7 doi:10.1016/j.fct.2008.07.003

Craft BD, Chiodini A, Garst J, Granvogl M (2013) Fatty acid esters of monochloropropanediol (MCPD) and glycidol in refined edible oils. Food additives & contaminants Part A, Chemistry, analysis, control, exposure & risk assessment 30(1):46-51 doi:10.1080/19440049.2012.709196

EFSA (2016) Risks for human health related to the presence of 3- and 2-monochloropropanediol (MCPD), and their fatty acid esters, and glycidyl fatty acid esters in food. EFSA Journal 14(5):4426 doi:10.2903/j.efsa.2016.4426

EFSA (2018) Update of the risk assessment on 3-monochloropropane diol and its fatty acid esters. EFSA Journal 16(1):5083 doi:10.2903/j.efsa.2018.5083

Elbirt KK, Whitmarsh AJ, Davis RJ, Bonkovsky HL (1998) Mechanism of sodium arsenite-mediated induction of heme oxygenase-1 in hepatoma cells. Role of mitogen-activated protein kinases. J Biol Chem 273(15):8922-31

Ford WC, Waites GM (1982) Activities of various 6-chloro-6-deoxysugars and (S) alpha-chlorohydrin in producing spermatocoeles in rats and paralysis in mice and in inhibiting glucose metabolism in bull spermatozoa in vitro. J Reprod Fertil 65(1):177-83

Gong P, Stewart D, Hu B, Vinson C, Alam J (2002) Multiple basic-leucine zipper proteins regulate induction of the mouse heme oxygenase-1 gene by arsenite. Arch Biochem Biophys 405(2):265-74

IARC (2012) 3-Monochloro-1,2-propanediol IARC Monographs on the Evaluation of Carcinogenic Risks to Humans. IARC Press, Lyon, France 101:349-374
Jones AR, Milton DH, Murcott C (1978) The oxidative metabolism of alpha-chlorohydrin in the male rat and the formation of spermatocoeles. Xenobiotica 8(9):573-82 doi:10.3109/00498257809061257
Kim K, Song C, Park Y, et al. (2004) 3-monochloropropane-1,2-diol does not cause neurotoxicity in vitro or neurobehavioral deficits in rats. Neurotoxicology 25(3):377-85 doi:10.1016/j.neuro.2003.08.004
Kinumi T, Kimata J, Taira T, Ariga H, Niki E (2004) Cysteine-106 of DJ-1 is the most sensitive cysteine residue to hydrogen peroxide-mediated oxidation in vivo in human umbilical vein endothelial cells. Biochem Biophys Res Commun 317(3):722-8 doi:10.1016/j.bbrc.2004.03.110
Kuhlmann J (2011) Determination of bound 2,3-epoxy-1-propanol (glycidol) and bound monochloropropanediol (MCPD) in refined oils. Eur J Lipid Sci Tech 113(3):335-344 doi:DOI 10.1002/ejlt.201000313
Laemmli UK (1970) Cleavage of structural proteins during the assembly of the head of bacteriophage T4. Nature 227(5259):680-5
Lee BS, Park SJ, Kim YB, et al. (2015) A 28-day oral gavage toxicity study of 3-monochloropropane-1,2-diol (3-MCPD) in CB6F1-non-Tg rasH2 mice. Food and chemical toxicology : an international journal published for the British Industrial Biological Research Association 86:95-103 doi:10.1016/j.fct.2015.09.019
Luckert C, Ehlers A, Buhrke T, Seidel A, Lampen A, Hessel S (2013) Polycyclic aromatic hydrocarbons stimulate human CYP3A4 promoter activity via PXR. Toxicology letters 222(2):180-8 doi:10.1016/j.toxlet.2013.06.243
Luczaj W, Gegotek A, Skrzydlewska E (2017) Antioxidants and HNE in redox homeostasis. Free Radic Biol Med 111:87-101 doi:10.1016/j.freeradbiomed.2016.11.033
McMahon M, Ding S, Acosta-Jimenez LP, Frangova TG, Henderson CJ, Wolf CR (2018) Measuring in vivo responses to endogenous and exogenous oxidative stress using a novel haem oxygenase 1 reporter mouse. The Journal of physiology 596(1):105-127 doi:10.1113/jp274915
Sawada S, Oberemm A, Buhrke T, et al. (2015) Proteomic analysis of 3-MCPD and 3-MCPD dipalmitate toxicity in rat testis. Food and chemical toxicology : an international journal published for the British Industrial Biological Research Association 83:84-92 doi:10.1016/j.fct.2015.06.002
Sawada S, Oberemm A, Buhrke T, Merschenz J, Braeuning A, Lampen A (2016) Proteomic analysis of 3-MCPD and 3-MCPD dipalmitate-induced toxicity in rat kidney. Archives of toxicology 90(6):1437-48 doi:10.1007/s00204-015-1576-8
Scharmach E, Buhrke T, Lichtenstein D, Lampen A (2012) Perfluorooctanoic acid affects the activity of the hepatocyte nuclear factor 4 alpha (HNF4alpha). Toxicology letters 212(2):106-12 doi:10.1016/j.toxlet.2012.05.007
Wilson MA (2011) The role of cysteine oxidation in DJ-1 function and dysfunction. Antioxid Redox Signal 15(1):111-22 doi:10.1089/ars.2010.3481

Figure 1

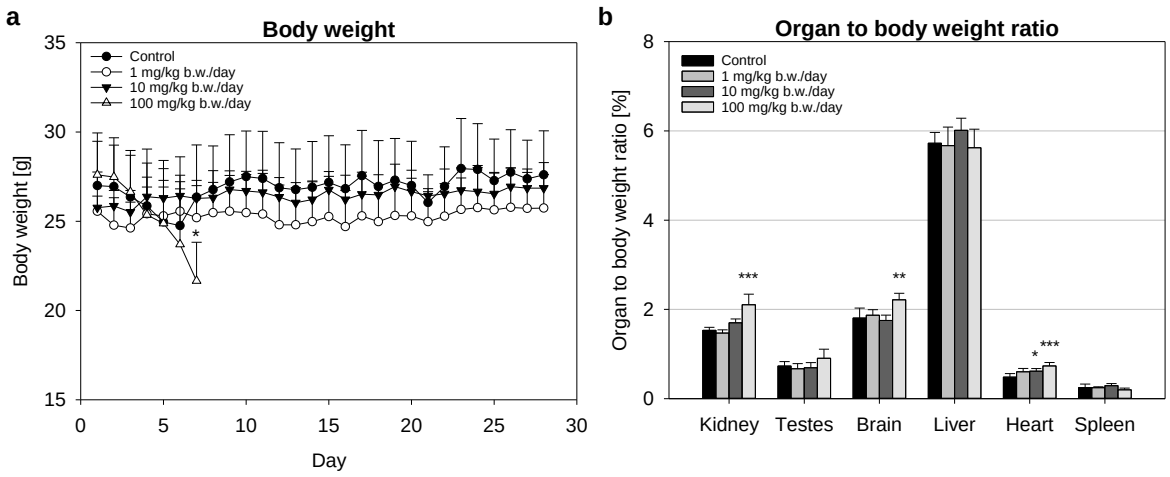
a
Body weight
Control
1 mg/kg b.w./day
10 mg/kg b.w./day
100 mg/kg b.w./day
Body weight [g]
Day
b
Organ to body weight ratio
Organ to body weight ratio [%]
Kidney
Testes
Brain
Liver
Heart
Spleen

Figure 2

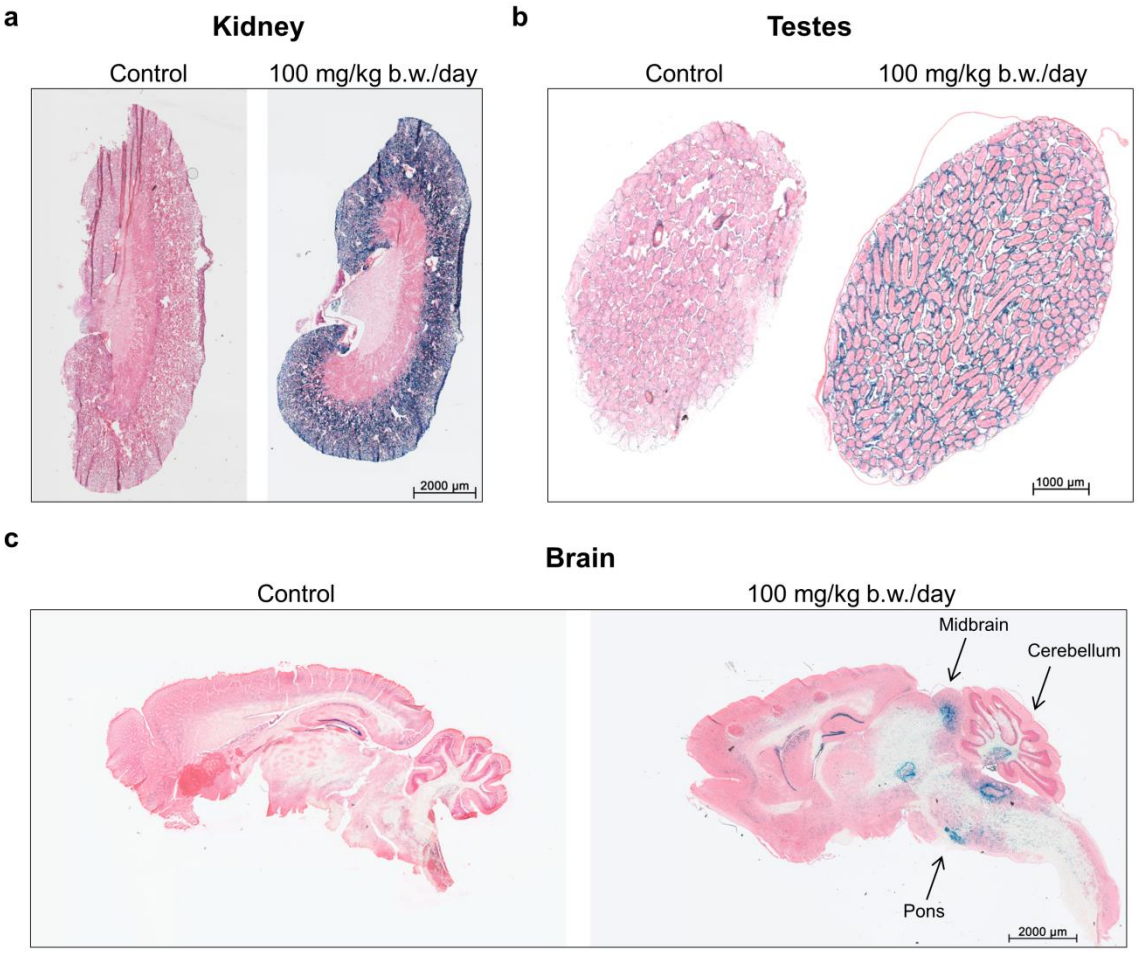
a
Kidney
Control
100 mg/kg b.w./day
2000 µm
b
Testes
Control
100 mg/kg b.w./day
1000 µm
c
Brain
Control
100 mg/kg b.w./day
Midbrain
Cerebellum
Pons
2000 µm

Figure 3

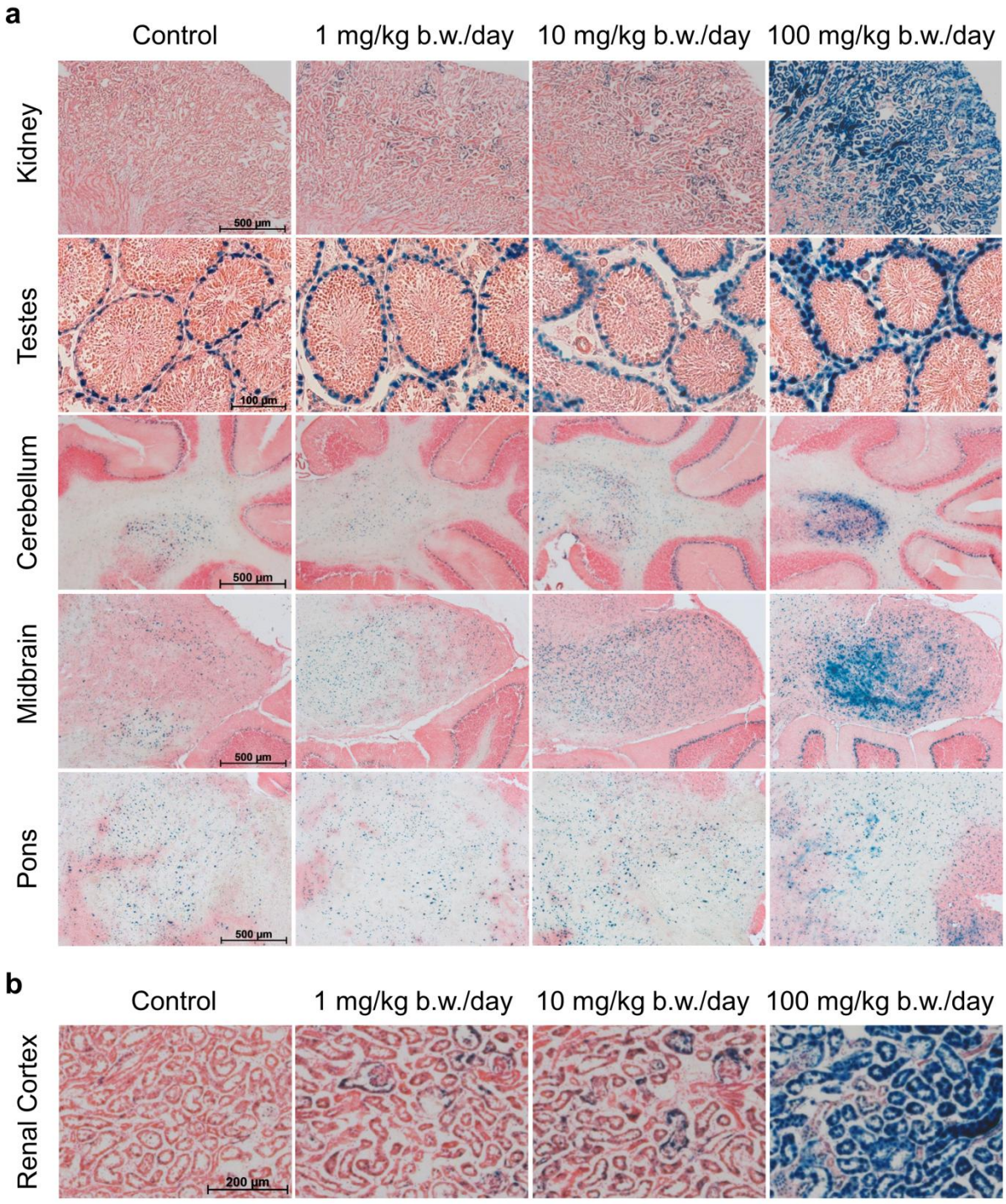
a
Control
1 mg/kg b.w./day
10 mg/kg b.w./day
100 mg/kg b.w./day
Kidney
Testes
Cerebellum
Midbrain
Pons
500 µm
100 µm
500 µm
500 µm
500 µm
b
Control
1 mg/kg b.w./day
10 mg/kg b.w./day
100 mg/kg b.w./day
Renal Cortex
200 µm

Figure 4

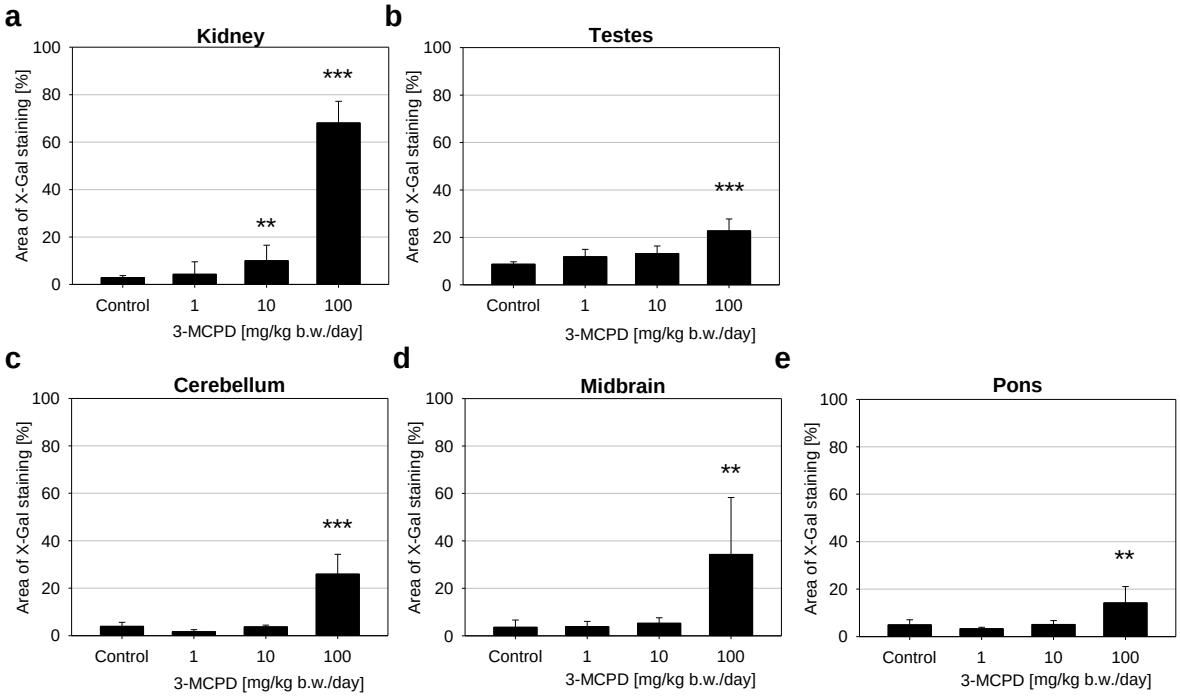
a
Kidney
Area of X-Gal staining [%]
100
80
60
40
20
0
**
***
Control
1
10
100
3-MCPD [mg/kg b.w./day]
b
Testes
Area of X-Gal staining [%]
***
Control
1
10
100
3-MCPD [mg/kg b.w./day]
c
Cerebellum
Area of X-Gal staining [%]
***
Control
1
10
100
3-MCPD [mg/kg b.w./day]
d
Midbrain
Area of X-Gal staining [%]
**
Control
1
10
100
3-MCPD [mg/kg b.w./day]
e
Pons
Area of X-Gal staining [%]
**
Control
1
10
100
3-MCPD [mg/kg b.w./day]

Figure 5

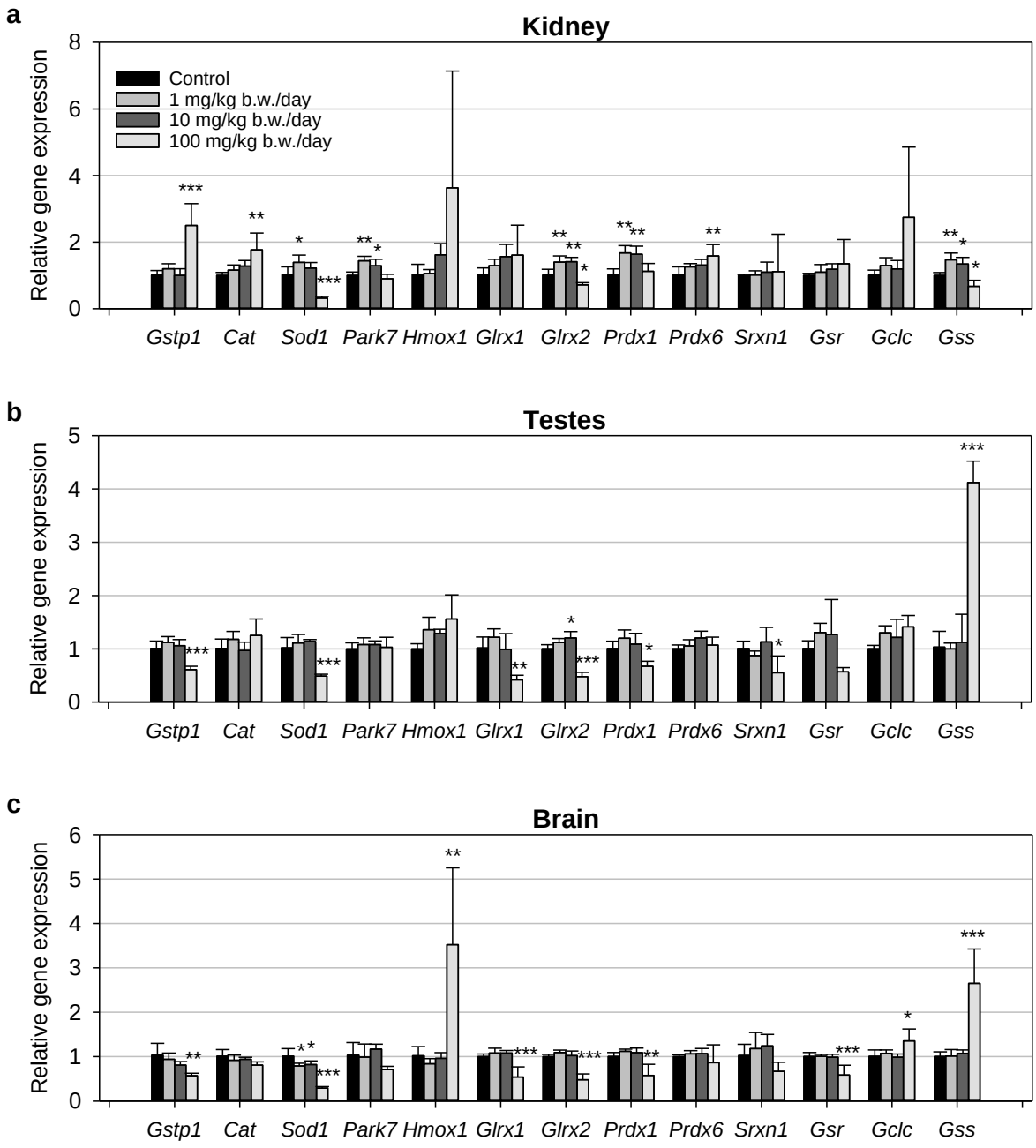
a
Kidney
Relative gene expression
Control
1 mg/kg b.w./day
10 mg/kg b.w./day
100 mg/kg b.w./day
Gstp1 Cat Sod1 Park7 Hmox1 Glrx1 Glrx2 Prdx1 Prdx6 Srxn1 Gsr Gclc Gss
b
Testes
Relative gene expression
Gstp1 Cat Sod1 Park7 Hmox1 Glrx1 Glrx2 Prdx1 Prdx6 Srxn1 Gsr Gclc Gss
c
Brain
Relative gene expression
Gstp1 Cat Sod1 Park7 Hmox1 Glrx1 Glrx2 Prdx1 Prdx6 Srxn1 Gsr Gclc Gss

Figure 6

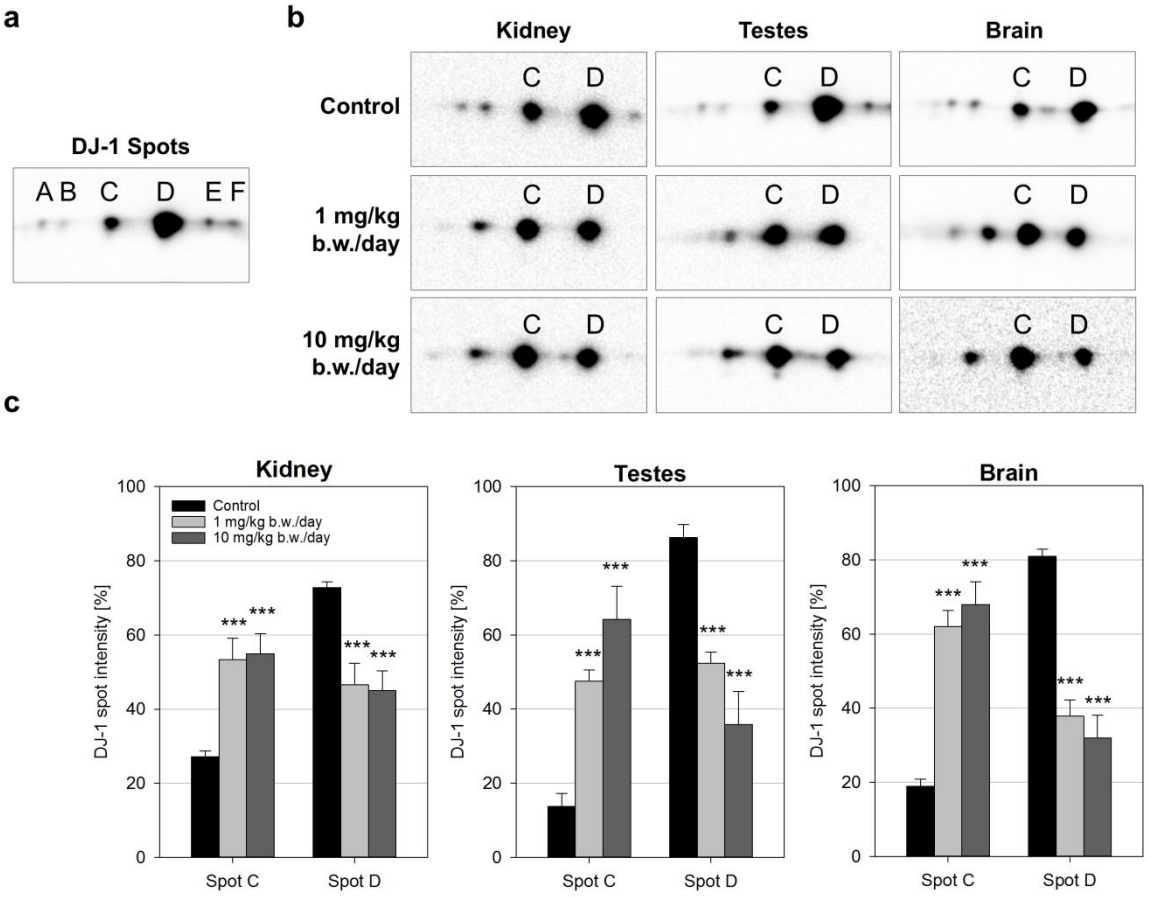
a
DJ-1 Spots
A B C D E F
b
Kidney
Testes
Brain
Control
1 mg/kg b.w./day
10 mg/kg b.w./day
C D
c
Kidney
Testes
Brain
Control
1 mg/kg b.w./day
10 mg/kg b.w./day
DJ-1 spot intensity [%]
Spot C
Spot D
***

Figure 7

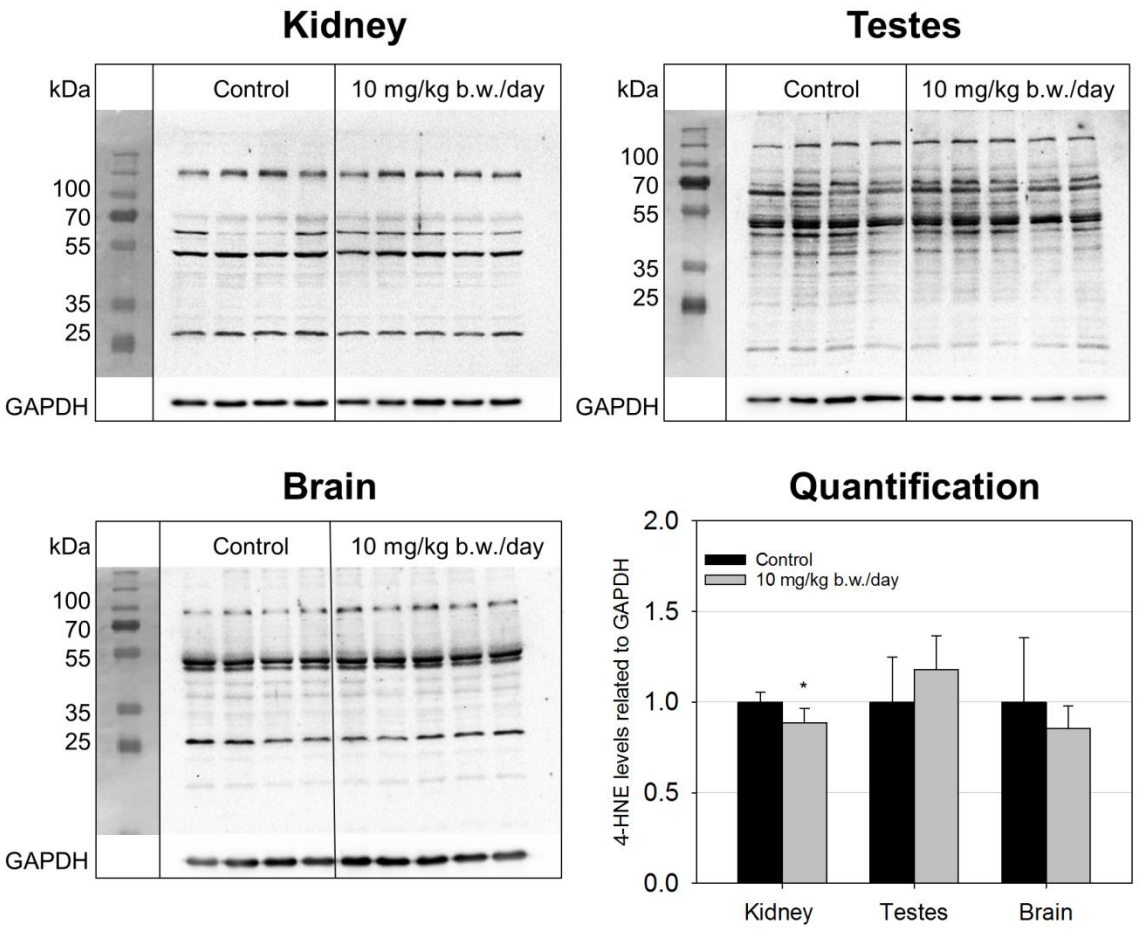
Kidney
kDa
Control
10 mg/kg b.w./day
100
70
55
35
25
GAPDH
Testes
kDa
Control
10 mg/kg b.w./day
100
70
55
35
25
GAPDH
Brain
kDa
Control
10 mg/kg b.w./day
100
70
55
35
25
GAPDH
Quantification
4-HNE levels related to GAPDH
Control
10 mg/kg b.w./day
2.0
1.5
1.0
0.5
0.0
*
Kidney
Testes
Brain

***Declaration of Interest Statement**

Declaration of interests

☒ The authors declare that they have no known competing financial interests or personal relationships that could have appeared to influence the work reported in this paper.

☐The authors declare the following financial interests/personal relationships which may be considered as potential competing interests: